# Qualitative analysis of a discrete fractional order prey-predator model: gompertz growth on prey with mixed functional responses

Md. Jasim Uddin[1*],Sarker Md. Sohel Rana[1]

[1] *Department of Mathematics, University of Dhaka, Dhaka-1000, Bangladesh*

*jasimu00@gmail.com,srana.mthdu@gmail.com*

[*] *corresponding author*

January 2, 2024

**Abstract**

We proposed a discrete fractional order predator-prey model that takes into account mixed functional responses of Holling type II and Ivlev in this study. The models fixed points are discovered, and their stability is assessed. We show analytically that the discrete model may sustain both bifurcations (Neimark-Sacker and Period doubling), which are key phenomena in discrete dynamical systems. We present the stability of NS and PD bifurcations using the central manifold theory. According to the modification of the control parameters, the dynamic behavior of this model is investigated. The key features of numerical simulations including bifurcation diagrams, maximal Lyapunov exponents, fractal dimensions (FD), and phase portraits are displayed to prove the accuracy of theoretical analysis as well as complex dynamical behaviors and richer and more intricate dynamics. It has been found that the parameter values significantly affect how the prey-predator model of fractional order behaves dynamically. In addition, two chaos management techniques are used to get rid of the chaos that the model objectively contains.

**Keywords:**Prey-predator model; Caputo fractional derivative; Period-Doubling(PD) and Neimark-Sacker (NS) Bifurcations; Fractal dimensions; Chaos control.

**Mathematics Subject Classification (2020):** 39A28; 39A30; 39A33; 70K50; 92D25.

## 1 Introduction

In population dynamics, continuous and discrete-time models are the two most popular types of mathematical frameworks. Numerous academics have recently argued that using difference equations to model the population dynamics model makes it more relevant and realistic [6, 14, 26, 43]. Discrete-time systems are more suitable for non-overlapping generations, such as annual plants or insect colonies with a single generation every year. Compared to their continuous-time counterparts in lower-dimensional systems, discrete models dynamics are richer and more complex. The more intricate patterns and chaotic behavior



**2 Jan 2024 08:51:36 PST**
**231108-MdJasim Version 2 - Submitted to Rocky Mountain J. Math.**

of nonlinear dynamics are best described by discrete systems.

Utilizing the forward Euler scheme with an integral step size is one method for discretizing a continuous system. Many studies have utilized this discretization scheme and varied as a bifurcation parameter, including Hadeler and Gerstmann [23], Salman et al. [43], Cheng and Cao [10], Hu and Cao [26], Liu and Xiao [33], Rana and Kulsum [41], Ajaz et al. [6] and many others. Din [14], Ishaque et al. [27], Khan [29], and the references therein used as an alternative discretization strategy for differential equations known as piecewise constant arguments. All the discretized systems demonstrated the existence and uniqueness of positive steady states, non-negativity and uniform boundedness of solution sets, and other properties that are challenging to demonstrate when using Eulers discretization approach. Recently, some authors have begun to employ the well-known Caputo fractional derivative in continuous models rather than conventional derivatives (we refer [1, 2, 5, 20, 49]). Since the prey-predator model works like conventional derivatives, fractional derivatives can be used. Because of this, the population's rate of change might be slower, which might result in a more accurate mathematical estimate. Differential and integral fractional calculus is frequently used to study complex system modeling in many scientific and engineering domains (see [13, 36, 37, 50, 51, 53]). In fractional calculus, the time domain is viewed as a memory effect in which the current state depends on its past history and the fractional order acts as a memory effect index in the time domain [45] or as a non-locality index in the space domain. In general, it is difficult to solve fractional differential equations (FDEs) analytically but it is possible to resolve these issues connected to FDEs numerically, as in [8, 17].

To comprehend the interactions between prey and predator, certain straightforward mathematical models have been proposed. The well known Lotka-Volterra model [34, 52], have been employed by population dynamics to comprehend the interaction between ecological species [4, 11, 12, 21, 32]. In a natural environment, each population has a different method to search for food sources and defend itself, such as rumination, grouping, etc. Numerous ecological features and elements are employed to build more accurate mathematical models. When it comes to population dynamics, the functional response is the ratio of a predator's prey intake to the density of prey per unit of time, which must be taken into consideration in every prey-predator contact. The Holling type IIs functional response is preferable to the Holling types I, III, and IVs responses with regard to the bulk of arthropod populations [25]. The Ivlev functional response which has a similar effect to Holling type IIs functional response was created by Ivlev [28] in order to research how prey and predator species interact dynamically. A discrete-time predator-prey system's dynamics with a functional response of Holling type III are discussed in [3] and in [31] Holling type-II response in a discrete-time phytoplankton-zooplankton model has been studied analytically and numerically, respectively. An explicit criterion for bifurcation analysis is presented for the 3D system in [42]. Modelling predator-prey interactions leveraging mixed functional responses studied in [18, 19, 47]. In [19, 47] the authors considered Holling type I and II functional responses whereas in [18] the authors considered mixed functional response to explore the complex dynamics in the system. If system solutions are chaotic, then it means that the predator-prey system is unstable, that is, if the prey is in chaotic, then the predator will ultimately tend to extinction, or tend to a chaotic. For chaotic



2 Jan 2024 08:51:36 PST
231108-MdJasim Version 2 - Submitted to Rocky Mountain J. Math.

dynamics and experimental results, we refer [24, 39]. The study in [48] thoroughly examines bifurcations, chaos analysis, and control in a discrete predator-prey model with mixed functional responses of Holling-I and Holling-II. Authors in [38] discussed several bifurcations of a discrete-time model of prey-predator dynamics with mixed functional responses. In predator-prey models, the functional response explains how the feeding rate of a predator varies with prey density. There are two primary forms of functional responses: the variable functional response and the adaptive functional response. Both variable and adaptive functional responses are important in influencing the dynamics of predator-prey interactions. This kind of functional response shown by a predator can affect the stability or instability of the predator-prey system. Adaptable reactions can incorporate more practical and intricate patterns into models, enabling a more accurate portrayal of how predators adapt their actions in response to variations in prey availability. To sum up, the decision between a variable and an adaptive functional response in a prey-predator model relies on the desired amount of detail and realism in the model. While variable responses record simple interactions, adaptive responses provide a more detailed picture of how predators alter their feeding rates based on their experiences and the current conditions in the environment.

This study attempts to explore the dynamics of a discrete fractional order prey-predator model with mixed Holling type-II and Ivlev functional responses. We thoroughly examine the proposed models fixed points local asymptotic stability. The bifurcation analysis at one of the control parameters for the model has been presented. Any one of these control factors can be altered to see how the models long-term behaviors change. In addition, we provide further numerical simulations to clarify and validate our analytical findings.

The rest of the paper is structured as follows. In Section 2, we present a discrete fractional order prey-predator model with functional responses of both Ivlev and Holling II. In Section 3, we look at the fixed point stability. In section 4, it is explored if Neimark-Sacker bifurcation exists around the coexistence fixed point of the system. The possibility of a PD bifurcation is discussed in section 5 at the discrete systems coexistence fixed point. In Section 6, we quantitatively depict model dynamics together with bifurcation visualisation, phase pictures, and MLEs to justify our mathematical observations. In Section 7, the FD predator and prey model uses the OGY and feedback technique to manage chaos. Short explanations are provided in Section 8.

## 2 Model Formulation

We assume that the densities of the prey and predator populations are constant across time, have a uniform distribution across space, and have no discernible stage structure for either the prey or the predators. The suggested model, which incorporates Gompertz growth into a generalized prey-predator model, is represented by the following differential equations:

$$\begin{aligned} \frac{dx}{dt} &= rx\ln\frac{k}{x} - \eta_c\varphi(x)y \\ \frac{dy}{dt} &= \beta_c\varphi(x)y - \delta_c y \end{aligned} \tag{1}$$



2 Jan 2024 08:51:36 PST
231108-MdJasim Version 2 - Submitted to Rocky Mountain J. Math.

Where the populations of prey and predators are represented by $x$ and $y$, respectively, at any time $t$. All the parameters $r, k, \eta_c, \beta_c,$ and $\delta_c$ are positive constants and have biological meanings that are consistent with this. The intrinsic growth rate of the prey population per person is $r$, the capacity of the environment is $k$, predators' highest rate of consumption per person is $\eta_c$, the efficiency at which prey is turned into new predators is $\beta_c$, and the per capita mortality rate of predators is $\delta_c$. The expression $\varphi(x)$ denotes the predator population's functional response and confirms the hypotheses $\varphi(0) = 0$, $\varphi^{'}(x) > 0$ for $x > 0$.

To analyses the system (1), we assume Holling type II functional response $\varphi(x) = \frac{\eta_c x}{\gamma_c + x}$ in the first equation and the Ivlev functional resonse $\varphi(x) = (1 - e^{-ax})$ in the second equation respectively. Following are the details of the predator-prey model with a mixed functional response.

$$\begin{aligned} \frac{dx}{dt} &= rx \ln \frac{k}{x} - \frac{\eta_c x}{\gamma_c + x} y \\ \frac{dy}{dt} &= \beta_c (1 - e^{-ax}) y - \delta_c y \end{aligned} \tag{2}$$

Researchers can obtain a more thorough knowledge of the dynamics involved in a prey-predator system by taking into account both Holling Type II and Ivlev Type functional responses. This is significant in a number of ways: realism, flexibility, predictive power, management and conservation, and so on. In addition, taking into account both Holling Type II and Ivlev type hybrid functional responses in a prey-predator system makes it possible to represent interactions between predator and prey species in a more accurate and nuanced way, taking into account the diverse behaviors and ecological traits of the various species involved.

A function $f(t)$'s Caputo fractional time derivative of order $\tau$ is given in [7],

$$D^{\tau} f(t) = \frac{1}{\Gamma(1-\tau)} \int_0^t \frac{1}{(t-\zeta)^{\tau}} f(\zeta)\, d\zeta, \tag{3}$$

where, $\tau \in (0, 1]$; $D^{\tau} = \frac{d^{\tau}}{dt^{\tau}}$, and $\Gamma(1-\tau)$ is the gamma function. As a result, the model (2)'s fractional-order form is provided as follows.

$$\begin{aligned} \frac{d^{\tau} x}{dt^{\tau}} &= D^{\tau} x = rx \ln \frac{k}{x} - \frac{\eta_c x}{\gamma_c + x} y \\ \frac{d^{\tau} y}{dt^{\tau}} &= D^{\tau} y = \beta_c (1 - e^{-ax}) y - \delta_c y \end{aligned} \tag{4}$$

Consider the initial approximations of system (4) are $x(0) = x_0, y(0) = y_0$. Then system (4) becomes:

$$\begin{aligned} \frac{d^{\tau} x}{dt^{\tau}} &= D^{\tau} x = rx([\frac{t}{\rho}]\rho) \ln \frac{k}{x([\frac{t}{\rho}]\rho)} - \frac{\eta_c x([\frac{t}{\rho}]\rho)}{\gamma_c + x([\frac{t}{\rho}]\rho)} y([\frac{t}{\rho}]\rho) \\ \frac{d^{\tau} y}{dt^{\tau}} &= D^{\tau} y = \beta_c (1 - e^{-ax([\frac{t}{\rho}]\rho)}) y([\frac{t}{\rho}]\rho) - \delta_c y([\frac{t}{\rho}]\rho) \end{aligned}$$

When $t \in [0, \rho)$, so $\frac{t}{\rho} \in [0, 1)$. So,

$$\frac{d^{\tau} x}{dt^{\tau}} = D^{\tau} x = rx_0 \ln \frac{k}{x_0} - \frac{\eta_c x_0}{\gamma_c + x_0} y_0$$



2 Jan 2024 08:51:36 PST
231108-MdJasim Version 2 - Submitted to Rocky Mountain J. Math.

$$\frac{d^\tau y}{dt^\tau} = D^\tau y = \beta_c(1-e^{-ax_0})y_0 - \delta_c y_0$$

After $n$ repetitions, we receive

$$x_{n+1}(t) = x_n(n\rho) + \frac{(t-n\rho)^\tau}{\Gamma(\tau+1)}\left(rx_n(n\rho)\ln\frac{k}{x_n(n\rho)} - \frac{\eta_c x_n(n\rho)}{\gamma_c + x_n(n\rho)}y_n(n\rho)\right),$$
$$y_{n+1}(t) = y_n(n\rho) + \frac{(t-n\rho)^\tau}{\Gamma(\tau+1)}\left(\beta_c(1-e^{-ax_n(n\rho)})y_n(n\rho) - \delta_c y_n(n\rho)\right).$$

where $t \in [n\rho, (n+1)\rho)$. For $t \longrightarrow (n+1)\rho$, system (2) becomes as in [50]

$$\begin{aligned} x_{n+1} &= x_n + \frac{\rho^\tau}{\Gamma(\tau+1)}\left(rx_n\ln\frac{k}{x_n} - \frac{\eta_c x_n}{\gamma_c + x_n}y_n\right), \\ y_{n+1} &= y_n + \frac{\rho^\tau}{\Gamma(\tau+1)}\left(\beta_c(1-e^{-ax_n})y_n - \delta_c y_n\right). \end{aligned} \tag{5}$$

The FD predator-prey system can be discretized using the Euler method is $\tau \to 1$ in (5). There are disadvantages and benefits to the FD discrete prey-predator model compared to the classical form. As the FD discrete prey-predator model is very new, there isn't much empirical data to support its applicability and accuracy. Analysis and solution of fractional-order difference equations are more difficult than with conventional discrete models. Standard model parameters are easier to determine, whereas FD parameters can be more unpredictable. Fractional order models can illuminate complicated systems with non-local interactions and memory effects despite these shortcomings. The primary themes of fractional calculus are derivatives and non-integer order integrals. Integer-order models are unable to capture complicated dynamics; fractional-order differential equations can. The discrete-time fractional prey-predator model (5) uses fractional calculus to offer a more adaptable and detailed portrayal of ecological dynamics. It takes into account memory effects and long-range dependencies that are not easily captured by classic models based on ordinary differential equations (ODEs). This method enables a more accurate representation of the evolutionary processes occurring between the species that interact with one another. The relationship between the time interval and ecological processes is crucial for comprehending the dynamics of prey-predator interactions. The time interval in a discrete-time prey-predator model is an important parameter that affects the temporal dynamics, accuracy, stability, and computational efficiency of the ecological simulation. Choosing a suitable time interval is crucial for achieving accurate and dependable outcomes when examining the dynamics of prey and predator populations across time.

# 3 Existence Conditions and the Stability Analysis of the Fixed Point

## 3.1 Existence of the fixed points

We only have two fixed points at most, depending on the situation.

(i) The axial fixed point $\kappa_1(k,0)$. Prey population approaches carrying capacity $k$ when there are no predators, according to biology.

(ii) The unique coexistence fixed point $\kappa_2(x^*, y^*)$, where $x^* = -\frac{\ln\left[1-\frac{\delta_c}{\beta_c}\right]}{a}, y^* = \frac{r(x^*+\gamma_c)\ln\left[\frac{k}{x^*}\right]}{\eta_c}$ exists if $\delta_c < \beta_c(1-e^{-ak})$.



2 Jan 2024 08:51:36 PST
231108-MdJasim Version 2 - Submitted to Rocky Mountain J. Math.

### 3.2 Local stability analysis of fixed points

At its designated fixed points, we evaluate the system (5)'s stability. Unaffected by the magnitude of the expected eigenvalues at the fixed point $\kappa(x,y)$, expected eigenvalues have an effect on the local stability of the fixed point, which is an important issue to notice.

$$V_b\left(x,y\right)=\begin{pmatrix} v\tilde{b_{11}} & v\tilde{b_{12}} \\ v\tilde{b_{21}} & v\tilde{b_{22}} \end{pmatrix} \tag{6}$$

where

$$\begin{aligned} v\tilde{b_{11}} &= 1+\left(\frac{r(x+\gamma_c)^2+y\gamma_c\eta_c}{(x+\gamma_c)^2}+r\ln[\frac{k}{x}]\right)\frac{\rho^\tau}{\Gamma(\tau+1)} \\ v\tilde{b_{12}} &= \left(-1+e^{-ax}\right)\eta\frac{\rho^\tau}{\Gamma(\tau+1)} \\ v\tilde{b_{21}} &= a\beta y e^{-ax}\frac{\rho^\tau}{\Gamma(\tau+1)} \\ v\tilde{b_{22}} &= 1+\left(-\delta+\beta-\gamma-e^{-ax}\beta\right)\frac{\rho^\tau}{\Gamma(\tau+1)} \end{aligned}$$

The jacobian matrix changes when we reach $\kappa_1(k,0)$

$$V_b\left(\kappa_1\right)=\begin{pmatrix} 1-r\frac{\rho^\tau}{\Gamma(\tau+1)} & \frac{-k\eta_c}{k+\gamma_c}\frac{\rho^\tau}{\Gamma(\tau+1)} \\ 0 & 1-\left(\delta_c-\beta_c(1-e^{-ak})\right)\frac{\rho^\tau}{\Gamma(\tau+1)} \end{pmatrix}.$$

The eigenvalues of $V_b\left(\kappa_1\right)$ are $\lambda_1=1-r\frac{\rho^\tau}{\Gamma(\tau+1)}$ and $\lambda_2=1-\left(\delta_c-\beta_c(1-e^{-ak})\right)\frac{\rho^\tau}{\Gamma(\tau+1)}$.

**Lemma 1.** *The topological classification listed below is suitable for the axial fixed point $\kappa_1$:*

*(i) if $\delta_c>\beta_c(1-e^{-ak})$ holds then $\kappa_1$ becomes*

*(i.i) sink if $0<\rho<min\{\left(\frac{2}{r}\Gamma(1+\tau)\right)^{\frac{1}{\tau}},\left(\frac{2}{\delta_c-\beta_c(1-e^{-ak})}\Gamma(1+\tau)\right)^{\frac{1}{\tau}}\}$,*

*(i.ii) source if $\rho>max\{\left(\frac{2}{r}\Gamma(1+\tau)\right)^{\frac{1}{\tau}},\left(\frac{2}{\delta_c-\beta_c(1-e^{-ak})}\Gamma(1+\tau)\right)^{\frac{1}{\tau}}\}$,*

*(i.iii) non-hyperbolic if $\rho=\left(\frac{2}{r}\Gamma(1+\tau)\right)^{\frac{1}{\tau}}$ or $\rho=\left(\frac{2}{\delta_c-\beta_c(1-e^{-ak})}\Gamma(1+\tau)\right)^{\frac{1}{\tau}}$,*

*(ii) if $\delta_c<\beta_c(1-e^{-ak})$ holds the fixed point $\kappa_1(k,0)$ becomes*

*(ii.i) If $\rho>\left(\frac{2}{r}\Gamma(1+\tau)\right)^{\frac{1}{\tau}}$ holds then $\kappa_1$ is source,*

*(ii.ii) saddle if $\rho<\left(\frac{2}{r}\Gamma(1+\tau)\right)^{\frac{1}{\tau}}$,*

*(ii.iii) non-hyperbolic if $\rho=\left(\frac{2}{r}\Gamma(1+\tau)\right)^{\frac{1}{\tau}}$,*

*(iii) if $\delta_c=\beta_c(1-e^{-ak})$ then the non-hyperbolic fixed point is $\kappa_1(k,0)$.*

It follows that $V_b\left(\kappa_1\right)$ has one eigenvalues is $-1$ as well as the alternative one not being equal to $\pm1$ when $\rho=\left(\frac{2}{r}\Gamma(1+\tau)\right)^{\frac{1}{\tau}}$ or $\rho=\left(\frac{2}{\delta_c-\beta_c(1-e^{-ak})}\Gamma(1+\tau)\right)^{\frac{1}{\tau}}$. Consequently, if parameters vary in a certain region around $\widehat{FB}^1_{\kappa_1}$ or $\widehat{FB}^2_{\kappa_1}$, a PD bifurcation may happen.

$$\widehat{FB}^1_{\kappa_1}=\left\{(r,a,k,\delta_c,\eta_c,\beta_c,\gamma_c,\rho,\tau)\in(0,+\infty):\rho=\left(\frac{2}{r}\Gamma(1+\tau)\right)^{\frac{1}{\tau}},\rho\neq\left(\frac{2}{\delta_c-\beta_c(1-e^{-ak})}\Gamma(1+\tau)\right)^{\frac{1}{\tau}}\right\},$$

or

$$\widehat{FB}^2_{\kappa_1}=\left\{(r,a,k,\delta_c,\eta_c,\beta_c,\gamma_c,\rho,\tau)\in(0,+\infty):\rho=\left(\frac{2}{\delta_c-\beta_c(1-e^{-ak})}\Gamma(1+\tau)\right)^{\frac{1}{\tau}},\rho\neq\left(\frac{2}{r}\Gamma(1+\tau)\right)^{\frac{1}{\tau}}\right\}.$$



**2 Jan 2024 08:51:36 PST**
**231108-MdJasim Version 2 - Submitted to Rocky Mountain J. Math.**

The characteristic equation changes when we reach $\kappa_2(x^*, y^*)$.

$$F_{22}(\lambda) := \lambda^2 - (2 + \tilde{\Delta_3}\tilde{\mu_b})\lambda + (1 + \tilde{\Delta_3}\tilde{\mu_b} + \tilde{\Omega_3}{\tilde{\mu_b}}^2) = 0 \tag{7}$$

where

$$\tilde{\Delta_3} = -r + \beta_c - e^{-ax^*}\beta_c - \delta_c + \frac{rx^* \ln[\frac{k}{x^*}]}{x^* + \gamma_c}$$

$$\tilde{\Omega_3} = \frac{e^{-ax^*}r}{(x^* + \gamma_c)}\left[-(x^* + \gamma_c)\left((-1 + e^{ax^*})\beta_c - e^{ax^*}\delta_c + x^*(\beta_c(-1 + e^{ax^*} + a(x^* + \gamma_c)) - e^{ax^*}\delta_c\right)\ln[\frac{k}{x^*}]\right]$$

So $F_{22}(1) = \tilde{\Omega_3}{\tilde{\mu_b}}^2 > 0$ and $F_{22}(-1) = 4 + 2\tilde{\Delta_3}\tilde{\mu_b} + \tilde{\Omega_3}{\tilde{\mu_b}}^2$. We derive the following lemma with respect to the stability criterion of $\kappa_2(x^*, y^*)$.

**Lemma 2.** *The topological categorization provided below is suitable for the coexistence fixed point $\kappa_2$:*

*(i) source when,*
*(i.i)* $\tilde{\Delta_3}^2 - 4\tilde{\Omega_3} \geq 0$ *and* $\tilde{\mu_b} > \frac{-\tilde{\Delta_3} + \sqrt{\tilde{\Delta_3}^2 - 4\tilde{\Omega_3}}}{\tilde{\Omega_3}}$
*(i.ii)* $\tilde{\Delta_3}^2 - 4\tilde{\Omega_3} < 0$ *and* $\tilde{\mu_b} > \frac{-\tilde{\Delta_3}}{\tilde{\Omega_3}}$
*(ii) sink if*
*(ii.i)* $\tilde{\Delta_3}^2 - 4\tilde{\Omega_3} \geq 0$ *and* $\tilde{\mu_b} < \frac{-\tilde{\Delta_3} - \sqrt{\tilde{\Delta_3}^2 - 4\tilde{\Omega_3}}}{\tilde{\Omega_3}}$
*(ii.ii)* $\tilde{\Delta_3}^2 - 4\tilde{\Omega_3} < 0$ *and* $\tilde{\mu_b} < \frac{-\tilde{\Delta_3}}{\tilde{\Omega_3}}$
*(iii) non-hyperbolic if*
*(iii.i)* $\tilde{\Delta_3}^2 - 4\tilde{\Omega_3} \geq 0$ *and* $\tilde{\mu_b} = \frac{-\tilde{\Delta_3} \pm \sqrt{\tilde{\Delta_3}^2 - 4\tilde{\Omega_3}}}{\tilde{\Omega_3}}; \tilde{\mu_b} \neq \frac{-2}{\tilde{\Delta_3}}, \frac{-4}{\tilde{\Delta_3}}$
*(iii.ii)* $\tilde{\Delta_3}^2 - 4\tilde{\Omega_3} < 0$ *and* $\tilde{\mu_b} = \frac{-4}{\tilde{\Delta_3}}$.
*(iv) saddle if otherwise*

Let,

$$\widehat{PDB}^{1,2}_{\kappa_2} = \left\{(r, a, k, \delta_c, \eta_c, \beta_c, \gamma_c, \rho, \tau) : \rho = \left(\frac{-\tilde{\Delta_3} \pm \sqrt{\tilde{\Delta_3}^2 - 4\tilde{\Omega_3}}}{\tilde{\Omega_3}}\Gamma(1 + \tau)\right)^{\frac{1}{\tau}} = \rho_{\pm},\right\}.$$

with $\tilde{\Delta_3}^2 - 4\tilde{\Omega_3} \geq 0, \tilde{\mu_b} \neq \frac{-2}{\tilde{\Delta_3}}, \frac{-4}{\tilde{\Delta_3}}$

The parameters $(r, a, k, \delta_c, \eta_c, \beta_c, \gamma_c, \rho, \tau)$ change within a constrained region of $\widehat{PDB}^{1,2}_{\kappa_2}$, causing the system (5) at $\kappa_2(x^*, y^*)$ to experience a PD bifurcation.

Also, let

$$\widehat{NSB}_{\kappa_2} = \left\{(r, a, k, \delta_c, \eta_c, \beta_c, \gamma_c, \rho, \tau) : \rho = \left(\Gamma(1 + \tau)\frac{-\tilde{\Delta_3}}{\tilde{\Omega_3}}\right)^{\frac{1}{\tau}} = \rho_{NS}, \tilde{\Delta_3}^2 - 4\tilde{\Omega_3} < 0\right\}.$$

If the parameters $(r, a, k, \delta_c, \eta_c, \beta_c, \gamma_c, \rho, \tau)$ vary around the set $\widehat{NSB}_{\kappa_2}$ , system (5) will suffer an NS bifurcation at that point.

The topological classification of the positive fixed point of the model (5) for $r = 2.5,\ \eta_c = 1.2,\ a = 0.25,\ \beta_c = 1.1,\ \delta_c = 0.1,\ \gamma_c = 0.5,\ \tau = 0.6$ in the $(\rho, K, a)-$ space in the window $[0, 5] \times [0, 3.5] \times [0.1, 0.55]$ is displayed in Figure 1(a). The green color-shaded segment presents the stability regions at the positive fixed point. For $a = 0.25$ the projection in 2D plane of the region in Figure 1(a) is decipted in Figure 1(b) with the PD curve and NS curve respectively.



**2 Jan 2024 08:51:36 PST**
**231108-MdJasim Version 2 - Submitted to Rocky Mountain J. Math.**

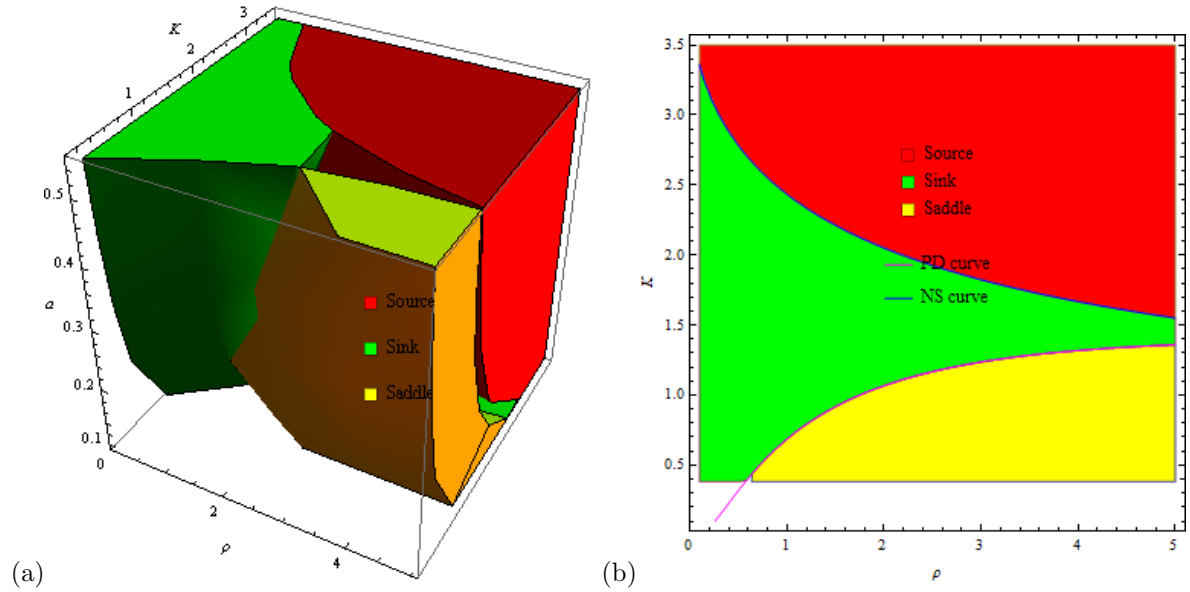


(a) (b)

Figure 1: (a)Positive steady state of model (5) in 3D topological classification (b) Region of stability (2D) of the model (5)'s positive steady state

## 4 Neimark Sacker Bifurcation Analysis at $\kappa_2(x^*, y^*)$

Here we investigate the NS bifurcation centered on the discrete model (5)'s sole positive stable situation. For this type of bifurcation's presence and direction, we have applied the conventional bifurcation theory. Several mathematicians have recently studied the NS bifurcation connected to several discrete-time mathematical systems [15, 16, 30]. Additionally, for specific considerations related to Hopf bifurcation when mathematical models are in differential form, (see[15, 44, 46]). First, we establish that whenever a specific parameter is selected as a bifurcation parameter, the positive equilibrium point $\kappa_2(x^*, y^*)$ of the system (5) undergoes the Neimark-Sacker bifurcation.

The parameter $\rho$ is utilised to study the NS bifurcation, and $\rho^*$ represents the perturbation.

$$\begin{aligned} x_{n+1} &= x_n + \frac{(\rho+\rho^*)^\tau}{\Gamma(\tau+1)}\left(rx_n \ln\frac{k}{x_n} - \frac{\eta_c x_n}{\gamma_c + x_n} y_n\right) \equiv f(x_n, y_n, \rho^*) \\ y_{n+1} &= y_n + \frac{(\rho+\rho^*)^\tau}{\Gamma(\tau+1)}\left(\beta_c(1-e^{-ax_n})y_n - \delta_c y_n\right) \equiv g(x_n, y_n, \rho^*) \end{aligned} \tag{8}$$

Where $|\rho^*| \lll 1$.

If $u_n = x_n - x^*, v_n = y_n - y^*$, then the fixed point $\kappa_2(x^*, y^*)$ becomes the origin and the model (8) becomes as the Taylor series at $(u_n, v_n) = (0, 0)$.

$$\begin{aligned} u_{n+1} &= \theta_{x1}u_n + \theta_{x2}v_n + \theta_{x11}u_n^2 + \theta_{x12}u_nv_n + \theta_{x22}v_n^2 + \theta_{x111}u_n^3 + \theta_{x112}u_n^2v_n + \\ &\quad \theta_{x122}u_nv_n^2 + \theta_{x222}v_n^3 + O((|u_n| + |v_n|)^4) \\ v_{n+1} &= \vartheta_{y1}u_n + \vartheta_{y2}v_n + \vartheta_{y11}u_n^2 + \vartheta_{y12}u_nv_n + \vartheta_{y22}v_n^2 + \vartheta_{y111}u_n^3 + \vartheta_{y112}u_n^2v_n + \\ &\quad \vartheta_{y122}u_nv_n^2 + \vartheta_{y222}v_n^3 + O((|u_n| + |v_n|)^4) \end{aligned} \tag{9}$$



2 Jan 2024 08:51:36 PST
231108-MdJasim Version 2 - Submitted to Rocky Mountain J. Math.

where

$$
\begin{aligned}
\theta_{x1} &= 1 - r\frac{\rho^\tau}{\Gamma(\tau+1)} + \frac{rx^*\frac{\rho^\tau}{\Gamma(\tau+1)}\ln\left[\frac{k}{x^*}\right]}{x^*+\gamma_c},\\
\theta_{x2} &= -\frac{x^*\eta_c\frac{\rho^\tau}{\Gamma(\tau+1)}}{x^*+\gamma_c},\\
\theta_{x11} &= -\frac{r\frac{\rho^\tau}{\Gamma(\tau+1)}\left((x^*+\gamma_c)^2 - 2x^*\gamma_c\ln\left[\frac{k}{x^*}\right]\right)}{x^*(x^*+\gamma_c)^2},\\
\theta_{x12} &= -\frac{\gamma_c\eta_c\frac{\rho^\tau}{\Gamma(\tau+1)}}{(x^*+\gamma_c)^2},\\
\theta_{x22} &= 0,\\
\theta_{x111} &= -\frac{r\frac{\rho^\tau}{\Gamma(\tau+1)}\left((x^*+\gamma_c)^3 - 6x^{*2}\gamma_c\ln\left[\frac{k}{x^*}\right]\right)}{x^{*2}(x^*+\gamma_c)^3},\\
\theta_{x112} &= \frac{2\gamma_c\eta_c\frac{\rho^\tau}{\Gamma(\tau+1)}}{(x^*+\gamma_c)^3},\\
\theta_{x122} &= 0,\\
\theta_{x222} &= 0,\\
\vartheta_{y1} &= \frac{ae^{-ax^*}r\beta_c(x^*+\gamma_c)\frac{\rho^\tau}{\Gamma(\tau+1)}\ln\left[\frac{k}{x^*}\right]}{\eta_c},\\
\vartheta_{y2} &= 1 - \delta_c\frac{\rho^\tau}{\Gamma(\tau+1)} + \beta_c\left(\frac{\rho^\tau}{\Gamma(\tau+1)} - e^{-ax^*}\frac{\rho^\tau}{\Gamma(\tau+1)}\right),\\
\vartheta_{y11} &= \frac{a^2e^{-ax^*}r\beta_c(x^*+\gamma_c)\frac{\rho^\tau}{\Gamma(\tau+1)}\ln\left[\frac{k}{x^*}\right]}{\eta_c},\\
\vartheta_{y12} &= ae^{-ax^*}\beta_c\frac{\rho^\tau}{\Gamma(\tau+1)},\\
\vartheta_{y22} &= 0,\\
\vartheta_{y111} &= \frac{a^3e^{-ax^*}r\beta_c(x^*+\gamma_c)\frac{\rho^\tau}{\Gamma(\tau+1)}\ln\left[\frac{k}{x^*}\right]}{\eta_c},\\
\vartheta_{y112} &= -a^2e^{-ax^*}\beta_c\frac{\rho^\tau}{\Gamma(\tau+1)},\\
\vartheta_{y122} &= 0,\\
\vartheta_{y222} &= 0.
\end{aligned}
\tag{10}
$$

When system (9)'s jacobian matrix is constructed at $(0,0)$, the following equation results:

$$\lambda^2 + \tilde{\chi_c}(\rho^*)\lambda + \tilde{\chi_d}(\rho^*) = 0$$

where

$$
\begin{aligned}
\tilde{\chi_c}(\rho^*) &= 2 + \tilde{\Delta_3}\tilde{\mu_b},\\
\tilde{\chi_d}(\rho^*) &= 1 + \tilde{\Delta_3}\tilde{\mu_b} + \tilde{\Omega_3}{\tilde{\mu_b}}^2,\\
\tilde{\mu_b} &= \frac{(\rho+\rho^*)^\tau}{\Gamma(\tau+1)}
\end{aligned}
$$

Following that, the complex solutions are determined as follows:
$\lambda_{1,2}(\rho^*) = \frac{-\tilde{\chi_c}(\rho^*)\pm i\sqrt{4\tilde{\chi_d}(\rho^*)-(\tilde{\chi_c}(\rho^*))^2}}{2}$.



**2 Jan 2024 08:51:36 PST**
**231108-MdJasim Version 2 - Submitted to Rocky Mountain J. Math.**

The eigenvalues of $\kappa_2$ are two complex conjugate numbers with modulus 1. We have $|\lambda_{1,2}(\rho^*)| = [\tilde{\chi_d}(\rho^*)]^{\frac{1}{2}}$ and

$l = \left[\frac{d|\lambda_{1,2}(\rho^*)|}{d\rho^*}\right]_{\rho^*=0} = \frac{\tilde{l_{aa}}}{\tilde{l_{bb}}} \neq 0.$

where

$$\tilde{l_{aa}} = e^{-ax^*}\left(-(x^*+\gamma_c)(\beta_c - 2r\beta_c\frac{\rho^\tau}{\Gamma(\tau+1)} + e^{ax^*}(r-\beta_c+\delta_c+(2r\beta_c-2r\delta_c)\frac{\rho^\tau}{\Gamma(\tau+1)}))\right),$$
$$+ e^{-ax^*}\left(rx^*(2\beta_c(-1+a(x^*+\gamma))\frac{\rho^\tau}{\Gamma(\tau+1)}) + e^{ax^*}(1+2(\beta_c-\delta_c)\frac{\rho^\tau}{\Gamma(\tau+1)})\ln\left[\frac{k}{x^*}\right]\right),$$
$$\tilde{l_{bb}} = 2(x^*+\gamma_c)\sqrt{\frac{e^{-ax^*}(-(x^*+\gamma_c)(-1+r\frac{\rho^\tau}{\Gamma(\tau+1)})(-\beta_c\frac{\rho^\tau}{\Gamma(\tau+1)} + e^{ax^*}(1+(\beta_c-\delta_c)\frac{\rho^\tau}{\Gamma(\tau+1)})))}{x^*+\gamma_c}},$$
$$+ 2(x^*+\gamma_c)\sqrt{\frac{e^{-ax^*}(rx^*\frac{\rho^\tau}{\Gamma(\tau+1)}(\beta_c(-1+a(x^*+\gamma))\frac{\rho^\tau}{\Gamma(\tau+1)} + e^{ax^*}(1+(\beta_c-\delta_c)\frac{\rho^\tau}{\Gamma(\tau+1)}))\ln\left[\frac{k}{x^*}\right])}{x^*+\gamma_c}},$$

Furthermore, it is crucial that when $\rho^* = 0$, $\lambda_{1,2}^j \neq 1$, $j = 1,2,3,4$, that is identical to $\tilde{\chi_c}(0) \neq \pm 2, 0, 1$. Set $\phi = Im(\lambda_{1,2})$ and $\varphi = Re(\lambda_{1,2})$. We establish $T = \begin{bmatrix} 0 & 1 \\ \phi & \varphi \end{bmatrix}$, and using $\begin{bmatrix} u_n \\ v_n \end{bmatrix} = T \begin{bmatrix} \overline{x}_n \\ \overline{y}_n \end{bmatrix}$, the model (8) becomes

$$\begin{aligned} \overline{x}_{n+1} &= \varphi\overline{x}_n - \phi\overline{y}_n + f_{x11}(\overline{x}_n, \overline{y}_n) \\ \overline{y}_{n+1} &= \phi\overline{x}_n + \varphi\overline{y}_n + g_{y11}(\overline{x}_n, \overline{y}_n), \end{aligned} \tag{11}$$

where the terms in the model (11) for the variables $(\overline{x}_n, \overline{y}_n)$ with the order at least two are denoted, respectively, by the functions $f_{x11}$ and $g_{y11}$.

The following discriminating amount $\Omega_{ll}$ must be nonzero in order to pass through NSB:

$\Omega_{ll} = -Re\left[\frac{(1-2\overline{\lambda})\overline{\lambda}^2}{1-\lambda}\xi_{11}\xi_{20}\right] - \frac{1}{2}|\xi_{11}|^2 - |\xi_{02}|^2 + Re(\overline{\lambda}\xi_{21}),$

where

$$\xi_{20} = \frac{\varphi}{8}(2\vartheta_{y22} - \varphi\theta_{x22} - \theta_{x12} + 4\phi\theta_{x22} + i(4\phi\theta_{x22} - 2\theta_{x22} - 2\varphi\theta_{x22})) + \frac{\phi}{4}\theta_{x12}$$
$$+ i\frac{1}{8}(4\phi\vartheta_{y22} + 2\phi^2\theta_{x22} - 2\theta_{x11}) + \frac{\vartheta_{y12}}{8} + \frac{\varphi\theta_{x11} - 2\vartheta_{y11} + \varphi^3\theta_{x22} - \varphi^2\vartheta_{y22} - \varphi^2\theta_{x12} + \varphi\vartheta_{y12}}{4\phi},$$
$$\xi_{11} = \frac{\phi}{2}(\vartheta_{y22} - \varphi\theta_{x22}) + i\frac{1}{2}(\phi^2\theta_{x22} + \theta_{x11} + \varphi\theta_{x12} + \varphi^2\theta_{x22})$$
$$+ \frac{\vartheta_{y11} - \varphi\theta_{x11} + \varphi\vartheta_{y12} - \varphi^2\theta_{x12} - 2\varphi^2\vartheta_{y22} + 2\varphi^3\theta_{x22}}{2\phi},$$
$$\xi_{02} = \frac{1}{4}\phi(2\varphi\theta_{x22} + \theta_{x12} + \vartheta_{y22}) + i\frac{1}{4}(\vartheta_{y12} + 2\varphi\vartheta_{y22} - 2\varphi\theta_{x12} - \theta_{x11})$$
$$- \frac{\vartheta_{y11} - \varphi\theta_{x11} + \varphi\vartheta_{y12} - \varphi^2\theta_{x12} + \varphi^2\vartheta_{y22} - \varphi^3\theta_{x22}}{4\phi} + \frac{1}{4}\theta_{x22}i(\phi^2 - 3\varphi^2),$$
$$\xi_{21} = \frac{3}{8}\vartheta_{y222}(\phi^2+\varphi^2) + \frac{\vartheta_{y112}}{8} + \frac{\varphi}{4}\theta_{x112} + \frac{\varphi}{4}\vartheta_{y122} + \theta_{x122}(\frac{\phi^2}{8} + \frac{3\varphi^2}{8} - \frac{\varphi}{4})$$
$$+ \frac{3}{8}\theta_{x111} + i\frac{3}{8}\theta_{x222}(\phi^2+2\varphi^2) + i\frac{3\phi\varphi}{8}\theta_{x122} - \frac{1}{8}\vartheta_{y122}\phi i - i\frac{3\phi\varphi}{8}\vartheta_{y222} - i\frac{3\vartheta_{y111} - 3\varphi\theta_{x111}}{8\phi}$$
$$- i\frac{3\varphi\vartheta_{y112} - 3\varphi^2\alpha_{x112}}{8\phi} - i\frac{3\varphi^2\vartheta_{y122} - 3\varphi^3\theta_{x122}}{8\phi} - i\frac{3\varphi^3\vartheta_{y222} - 3\varphi^4\theta_{x222}}{8\phi}.$$

As a result, we may prove the following theorem concerning Neimark-Sacker bifurcation's presence at the fixed point of the system (5) (see [[22, 44, 46, 54]]).



**2 Jan 2024 08:51:36 PST**
**231108-MdJasim Version 2 - Submitted to Rocky Mountain J. Math.**

**Theorem 1.** *At the coexistence equilibrium point $\kappa_2(x^*, y^*)$ if and only if $\Omega_{ll} = 0$, system (5) experiences a Neimark-Sacker bifurcation. Furthermore, an unique closed invariant curve bifurcating from $\kappa_2(x^*, y^*)$ exists and is asymptotically stable (respectively unstable) if $\Omega_{ll} < 0$ (or $\Omega_{ll} > 0$).*

# 5 Period-doubling bifurcation at $\kappa_2(x^*, y^*)$

Here we investigate the PD bifurcation centered on the discrete model (5)'s sole positive stable situation. After displaying the presence and direction of this type of bifurcation using normal forms, to investigate it, the center manifold theorem is employed. Recent research has been done by several scientists on the PD bifurcation in discrete-time models [22, 46, 54]. If the model's parameters vary around the set $\widehat{PDB}^{1,2}_{\kappa_2}$, then the positive steady state $\kappa_2$ has strictly $\lambda_1 = -1$ and $\lambda_2$ is 1 or $-1$.

The parameter $\rho$ is utilized to study the PD bifurcation, and $\rho^*$ represents the perturbation.

$$\begin{aligned} x_{n+1} &= x_n + \frac{(\rho+\rho^*)^\tau}{\Gamma(\tau+1)}\left(r x_n \ln\frac{k}{x_n} - \frac{\eta_c x_n}{\gamma_c + x_n} y_n\right) \equiv f(x_n, y_n, \rho^*) \\ y_{n+1} &= y_n + \frac{(\rho+\rho^*)^\tau}{\Gamma(\tau+1)}\left(\beta_c(1-e^{-a x_n}) y_n - \delta_c y_n\right) \equiv g(x_n, y_n, \rho^*) \end{aligned} \tag{12}$$

Where $|\rho^*| \lll 1$.

If $u_n = x_n - x^*, v_n = y_n - y^*$, then the fixed point $\kappa_2$ becomes the origin and the model (12) becomes as the Taylor series at $(u_n, v_n) = (0, 0)$.

$$\begin{aligned} u_{n+1} &= \theta_{x1}u_n + \theta_{x2}v_n + \theta_{x11}u_n^2 + \theta_{x12}u_n v_n + \theta_{x13}u_n\rho^* + \theta_{x23}v_n\rho^* + \theta_{x111}u_n^3 + \\ &\quad \theta_{x112}u_n^2 v_n + \theta_{x113}u_n^2\rho^* + \theta_{x123}u_n v_n\rho^* + O((|u_n| + |v_n| + |\rho^*|)^4) \\ v_{n+1} &= \vartheta_{y1}u_n + \vartheta_{y2}v_n + \vartheta_{y11}u_n^2 + \vartheta_{y12}u_n v_n + \vartheta_{y22}v_n^2 + \vartheta_{y13}u_n\rho^* + \vartheta_{y23}v_n\rho^* + \vartheta_{y111}u_n^3 + \\ &\quad \vartheta_{y112}u_n^2 v_n + \vartheta_{y113}u_n^2\rho^* + \vartheta_{y123}u_n v_n\rho^* + \vartheta_{y223}v_n^2\rho^* + O((|u_n| + |v_n| + |\rho^*|)^4), \end{aligned} \tag{13}$$

where

$$\begin{aligned} \alpha_{13} &= r\left(-1 + \frac{x^* \ln\left[\frac{k}{x^*}\right]}{x^* + \gamma_c}\right)\frac{\tau\rho^{\tau-1}}{\Gamma(\tau+1)}, \\ \alpha_{23} &= -\frac{x^*\eta_c}{x^* + \gamma_c}\frac{\tau\rho^{\tau-1}}{\Gamma(\tau+1)}, \\ \alpha_{113} &= -\frac{r\left((x^*+\gamma_c)^2 - 2x^*\gamma_c \ln\left[\frac{k}{x^*}\right]\right)}{x^*(x^*+\gamma_c)^2}\frac{\tau\rho^{\tau-1}}{\Gamma(\tau+1)}, \\ \alpha_{123} &= -\frac{\gamma_c\eta_c}{(x^*+\gamma_c)^2}\frac{\tau\rho^{\tau-1}}{\Gamma(\tau+1)}, \\ \beta_{13} &= \frac{a e^{-a x^*} r\beta_c(x^*+\gamma_c)\ln\left[\frac{k}{x^*}\right]}{\eta_c}\frac{\tau\rho^{\tau-1}}{\Gamma(\tau+1)}, \\ \beta_{23} &= (\beta_c(1-e^{-a x^*}) - \delta_c)\frac{\tau\rho^{\tau-1}}{\Gamma(\tau+1)}, \\ \beta_{113} &= -\frac{a^2 e^{-a x^*} r\beta_c(x^*+\gamma_c)\ln\left[\frac{k}{x^*}\right]}{\eta_c}\frac{\tau\rho^{\tau-1}}{\Gamma(\tau+1)}, \\ \beta_{123} &= a e^{-a x^*}\beta_c\frac{\tau\rho^{\tau-1}}{\Gamma(\tau+1)}, \end{aligned}$$



**2 Jan 2024 08:51:36 PST**
**231108-MdJasim Version 2 - Submitted to Rocky Mountain J. Math.**

$$\beta_{223} = 0. \tag{14}$$

We assume $T = \begin{bmatrix} \theta_{x2} & \theta_{x2} \\ -1-\theta_{x1} & \lambda_2-\theta_{x1} \end{bmatrix}$ that can be flipped. Utilizing the transformation now $\begin{bmatrix} u_n \\ v_n \end{bmatrix} = T \begin{bmatrix} \overline{x}_n \\ \overline{y}_n \end{bmatrix}$, then (13) becomes

$$\begin{aligned} \overline{x}_{n+1} &= -\overline{x}_n + f_{x11}(u_n, v_n, \rho^*) \\ \overline{y}_{n+1} &= \lambda_2 \overline{y}_n + g_{y11}(u_n, v_n, \rho^*), \end{aligned} \tag{15}$$

where the terms in the model (15) for the variables $(\overline{x}_n, \overline{y}_n)$ with the order at least two are denoted, respectively, by the functions $f_{x11}$ and $g_{y11}$.

The dynamics of the fixed point $\kappa_2$ at $\rho^* = 0$ are then determined by applying the center manifold theorem. A center manifold $V^c(0,0,0)$ of Map (15) exists. It can be stated this way:

$V^c(0,0,0) = \left\{(\overline{x}_n, \overline{y}_n, \rho^*)\, \epsilon R^3 : \overline{y}_{n+1} = \overline{\theta}_{x1}\overline{x}_n^2 + \overline{\theta}_{x2}\overline{x}_n\rho^* + O((|\overline{x}_n| + |\rho^*|)^3)\right\}$

where

$$\overline{\theta}_{x1} = \frac{\theta_{x2}[(1+\theta_{x1})\theta_{x11} + \theta_{x2}\vartheta_{y11}]}{1-\lambda_2^2} + \frac{\vartheta_{y22}(1+\theta_{x1})^2}{1-\lambda_2^2} - \frac{(1+\theta_{x1})[\theta_{x12}(1+\theta_{x1}) + \theta_{x2}\vartheta_{y12}]}{1-\lambda_2^2},$$
$$\overline{\theta}_{x2} = \frac{(1+\theta_{x1})[\theta_{x23}(1+\theta_{x1}) + \theta_{x2}\vartheta_{y23}]}{\theta_{x2}(1+\lambda_2)^2} - \frac{(1+\theta_{x1})[\theta_{x13} + \theta_{x2}\vartheta_{y13}]}{(1+\lambda_2)^2}.$$

The restrained center manifold $V^c(0,0,0)$ of the model (15) has the following structure:

$\overline{x}_{n+1} = -\overline{x}_n + h_1\overline{x}_n^2 + h_2\overline{x}_n\rho^* + h_3\overline{x}_n^2\rho^* + h_4\overline{x}_n\rho^{*2} + h_5\overline{x}_n^3 + O((|\overline{x}_n| + |\rho^*|)^3) \equiv F(\overline{x}_n, \rho^*)$

where



**2 Jan 2024 08:51:36 PST**
**231108-MdJasim Version 2 - Submitted to Rocky Mountain J. Math.**

$$
\begin{aligned}
h_1 &= \frac{\overline{\theta}_{x2}[(\lambda_2-\overline{\theta}_{x1})\theta_{x11}-\overline{\theta}_{x2}\vartheta_{y11}]}{1+\lambda_2}-\frac{\vartheta_{x22}(1+\overline{\theta}_{x1})^2}{1+\lambda_2}-\frac{(1+\overline{\theta}_{x1})[(\lambda_2-\overline{\theta}_{x1})\theta_{x12}-\overline{\theta}_{x2}\vartheta_{y12}]}{1+\lambda_2},\\
h_2 &= \frac{(\lambda_2-\overline{\theta}_{x1})\theta_{x13}-\overline{\theta}_{x2}\vartheta_{y13}}{1+\lambda_2}-\frac{(1+\overline{\theta}_{x1})[(\lambda_2-\overline{\theta}_{x1})\theta_{x23}-\overline{\theta}_{x2}\vartheta_{y23}]}{\overline{\theta}_{x2}\,(1+\lambda_2)},\\
h_3 &= \frac{(\lambda_2-\theta_{x1})\overline{\theta}_{x1}\theta_{x13}-\theta_{x2}\vartheta_{y13}}{1+\lambda_2}+\frac{[(\lambda_2-\theta_{x1})\theta_{x23}-\theta_{x2}\vartheta_{y23}](\lambda_2-\theta_{x1})\overline{\theta}_{x1}}{\theta_{x2}\,(1+\lambda_2)}\\
&\quad-\frac{(1+\theta_{x1})[(\lambda_2-\theta_{x1})\theta_{x123}-\theta_{x2}\vartheta_{y123}]}{1+\lambda_2}+\frac{\theta_{x2}[(\lambda_2-\theta_{x1})\theta_{x113}-\theta_{x2}\vartheta_{y113}]}{1+\lambda_2},\\
&\quad-\frac{\vartheta_{y223}(1+\theta_{x1})^2}{1+\lambda_2}+\frac{2\theta_{x2}\overline{\theta}_{x2}[(\lambda_2-\theta_{x1})\theta_{x11}-\theta_{x2}\vartheta_{y11}]}{1+\lambda_2},\\
&\quad-\frac{2\vartheta_{y22}\overline{\theta}_{x2}(1+\theta_{x1})(\lambda_2-\theta_{x1})}{1+\lambda_2}+\frac{\overline{\theta}_{x2}[(\lambda_2-\theta_{x1})\theta_{x12}-\theta_{x2}\vartheta_{y12}](\lambda_2-1-2\theta_{x1})}{1+\lambda_2},\\
h_4 &= \frac{\overline{\theta}_{x2}[(\lambda_2-\theta_{x1})\theta_{x13}-\theta_{x2}\vartheta_{y13}]}{1+\lambda_2}+\frac{[(\lambda_2-\theta_{x1})\theta_{x23}-\theta_{2}\vartheta_{x23}](\lambda_2-\theta_{x1})\overline{\theta}_{x2}}{\theta_{x2}\,(1+\lambda_2)}\\
&\quad+\frac{2\theta_{x2}\overline{\theta}_{x2}[(\lambda_2-\theta_{x1})\theta_{x11}-\theta_{x2}\vartheta_{y11}]}{1+\lambda_2},\\
&\quad+\frac{2\vartheta_{y22}\overline{\theta}_{x2}(1+\theta_{x1})(\lambda_2-\theta_{x1})}{1+\lambda_2}+\frac{\overline{\theta}_{x2}[(\lambda_2-\theta_{x1})\theta_{x12}-\theta_{x2}\vartheta_{y12}](\lambda_2-1-2\theta_{x1})}{1+\lambda_2},\\
h_5 &= \frac{2\theta_{x2}\overline{\theta}_{x1}[(\lambda_2-\theta_{x1})\theta_{x11}-\theta_{x2}\vartheta_{y11}]}{1+\lambda_2}+\frac{[(\lambda_2-\theta_{x1})\theta_{x11}-\theta_{x2}\vartheta_{y11}](\lambda_2-1-2\theta_{x1})\overline{\theta}_{x1}}{1+\lambda_2},\\
&\quad+\frac{2\vartheta_{y22}\overline{\theta}_{x1}(\lambda_2-\theta_{x1})(1+\theta_{x1})}{1+\lambda_2}+\frac{\overline{\theta}^2_{x2}[(\lambda_2-\theta_{x1})\theta_{x111}-\theta_{x2}\vartheta_{y111}]}{1+\lambda_2},\\
&\quad-\frac{\overline{\theta}_{x2}(1+\theta_{x1})[(\lambda_2-\theta_{x1})\theta_{x112}-\theta_{x2}\vartheta_{y112}]}{1+\lambda_2}.
\end{aligned}
$$

The next set of real numbers is as follows:

$H_{11}=\left(\frac{\partial^2 F}{\partial\overline{x}\partial\rho^*}+\frac{1}{2}\frac{\partial F}{\partial\rho^*}\frac{\partial^2 F}{\partial\overline{x}^2}\right)|_{(0,0)}$ and $H_{12}=\left(\frac{1}{6}\frac{\partial^3 F}{\partial\overline{x}^3}+\left(\frac{1}{2}\frac{\partial^2 F}{\partial\overline{x}^2}\right)^2\right)|_{(0,0)}$.

As a result of the earlier-mentioned investigation, we may infer the following finding regarding the existence and direction of period-doubling bifurcation for mathematical system (5).

**Theorem 2.** *For different values of $\rho$ in a constrained neighbourhood of $\widehat{PDB}^{1,2}_{\kappa_2}$, the model suffers PD bifurcation at $\kappa_2(x^*,y^*)$, if both $H_{11}$ and $H_{12}$ are not equal to zero. Furthermore, for $(H_{12}>0)$ $(H_{12}<0)$,it is stable (unstable) for the period-two orbits to split apart from $\kappa_2(x^*,y^*)$.*

# 6 Quantitative Study

Numerical simulation work has been done to display bifurcation diagrams, phase portraits, maximal Lyapunov exponents, and fractal dimension of the system (5) in order to validate our theoretical conclusions and highlight some unexpected, complicated dynamical patterns that are intriguing, present in the system (5). We take into account the bifurcation parameters in the following scenarios:

**Scenario (i):** The aforementioned parameter values were selected: $r=2.5,\ k=0.5,\ \eta_c=1.2,\ a=0.25,\ \beta_c=1.1,\ \delta_c=0.1,\ \gamma_c=0.5,\ \tau=0.6$ and $\rho$ varies between $0.6\le\rho\le 0.99$. We obtain a fixed point $\kappa_2(x^*,y^*)=(0.381241,0.497859)$ and PD bifurcation point at $\rho_+=0.719636$. The corresponding eigenvalues are $\lambda_{1,2}=-1,0.972735$. The model trajectory is shown in Figure 2 as changing how a steady state goes to a chaotic scenario via a PD bifurcation. The estimated MLEs and FDs for Figure 2(a-b) are shown in Figure 2(c-d). With regard to the bifurcation Figure 2, which essentially shows the bifurcation



2 Jan 2024 08:51:36 PST
231108-MdJasim Version 2 - Submitted to Rocky Mountain J. Math.

of a smooth, invariant closed curve into a chaotic attractor from a stable fixed point, the phase portraits are illustrated in Figure 3.

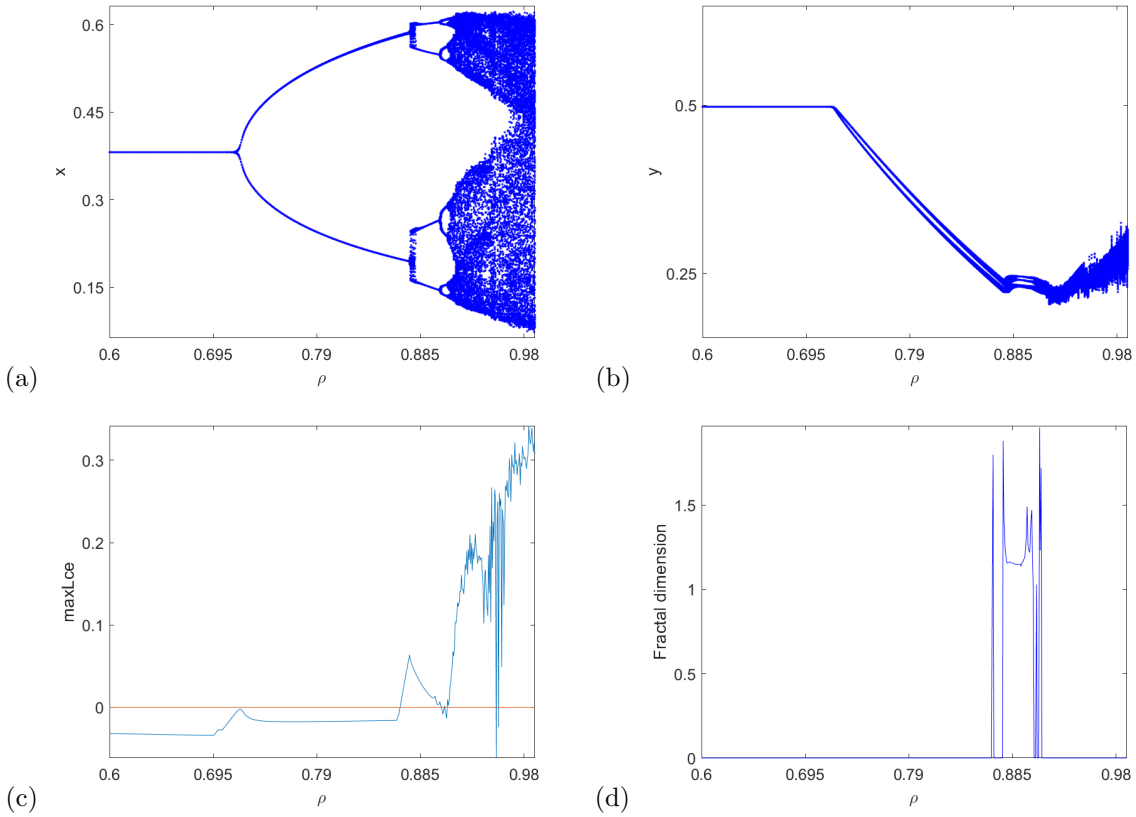


Figure 2: Visualisation of PD Bifurcation, MLEs, and FDs of species for changing parameter $\rho$

**Scenario (ii):** It was decided to use the following parameter values: $r = 2.5,\ k = 2.65,\ \eta_c = 1.2,\ a = 0.25,\ \beta_c = 1.1,\ \delta_c = 0.1,\ \gamma_c = 0.5,\ \tau = 0.6$ and $\rho$ varies between $0.5 \leq \rho \leq 1.19$. We obtain a fixed point $\kappa_2(x^*, y^*) = (0.381241, 3.55963)$ and bifurcation point at $\rho_{NS} = 0.66015$. The corresponding eigenvalues are $\lambda_{1,2} = 0.82422 \pm 0.566269$. The model trajectory is shown in Figure 4 as changing how a steady state goes to a chaotic scenario via an NS bifurcation. The phase portrait, Maximum Lyapunov exponents, and FD of Figure 4 (a-b) are depicted in Fig. 5 and Fig. 4 (c-d), consequently. There are three different periodic windows in each of the bifurcation processes for both prey and predator.

Figure 6 provides the orbit diagram of the prey and predator populations, along with other fixed parameter values: $r = 2.5,\ k = 2.65,\ \eta_c = 1.2,\ \rho = 0.8,\ \beta_c = 1.1,\ \delta_c = 0.1,\ \gamma_c = 0.5,\ \tau = 0.6$ and $a$ varies between $0.1 \leq a \leq 0.5$. We observe that the system passes through two NS bifurcation points are $a_{NS} = 0.203603, 0.47917$. Figure 6 shows the appropriate NS bifurcation visualisation, Maximum Lyapunov exponents, and Fractal dimensions.

If other values change (for example, parameter $\tau,\ k$), the discrete model in the NS visualization might act more significantly. The values of the parameters are set to construct a new NS bifurcation diagram as: $r = 2.5,\ k = 2.65,\ \eta_c = 1.2,\ a = 0.25,\ \beta_c = 1.1,\ \delta_c = 0.1,\ \gamma_c = 0.5,\ \rho = 0.66015$ and $\tau$ varies between $0 \leq \tau \leq 0.99$, as illustrated in Figure 7 (a-b). There is a Neimark-Sacker bifurcation in the model at



**2 Jan 2024 08:51:36 PST**
**231108-MdJasim Version 2 - Submitted to Rocky Mountain J. Math.**

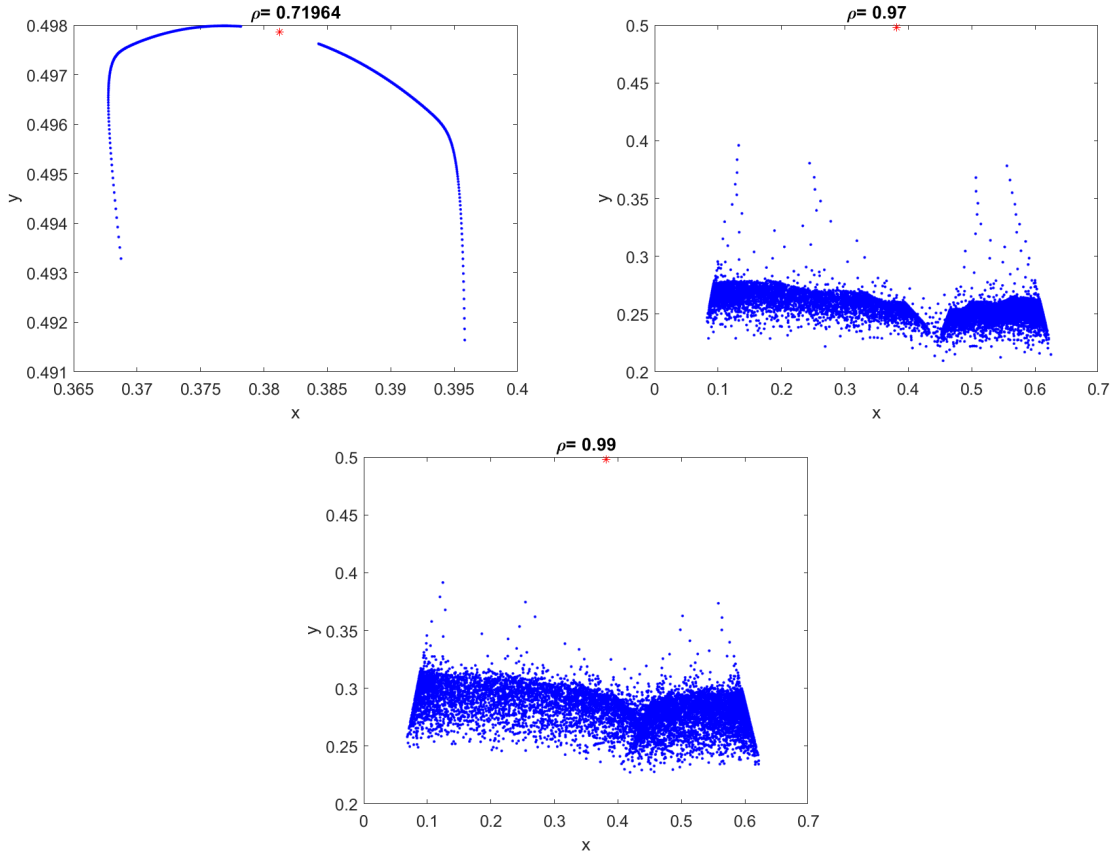


Figure 3: The phase diagram for altering the input of $\rho$

$\tau_{NS} = 0.6$. The MLEs and FDs corresponding to Figure 7 (a-b) are shown in Figure 7 (c-d). When the parameter values are set as $r = 2.5,\ \tau = 0.6,\ \eta_c = 1.2,\ a = 0.25,\ \beta_c = 1.1,\ \delta_c = 0.1,\ \gamma_c = 0.5,\ \rho = 0.66015$ and $k$ varies between $0.352 \leq \tau \leq 2.812$, , another NS bifurcation diagram is created as well, as illustrated in Figure (8) (a-b). Figure 9 (a) represents the two-parameter bifurcation diagrams in $(k, \rho, x)$-space. Figure 9 (b) displays the plot of two control parameter's maximal Lyapunov exponents onto the $(k, \rho)$ plane.

## 6.1 Biological Implications.

Bifurcations in discrete prey-predator models can have significant ecological consequences. These models explain the relationships between a group of animals that are hunted and another group of animals that do the hunting. In these models, the animals that are hunted are eaten by the animals who do the hunting.

Period-doubling bifurcations and Neimark-Sacker bifurcations are phenomena seen in dynamical systems, including ecological models. These divisions have significant biological consequences and can offer an understanding of the stability and intricacy of ecological systems. Period-doubling bifurcations are defined by the doubling of the oscillation period in population dynamics, which can have significant ecological consequences. Period-doubling bifurcations frequently indicate the shift from consistent, recurring patterns to unpredictable dynamics in a system. Within the framework of ecological models, this shift could suggest a decrease in the ability to make accurate predictions and the appearance of intricate, unpredictable changes in population levels. Period-doubling bifurcations are linked to the formation of periodic

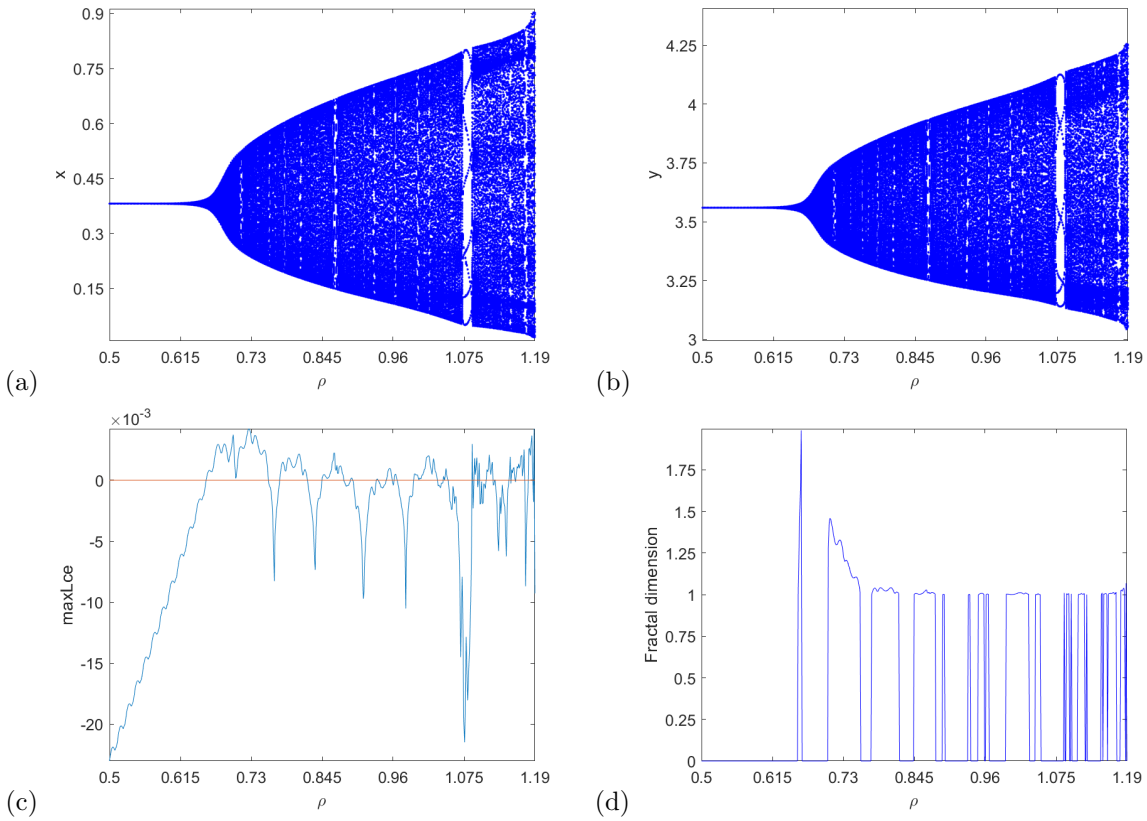


Figure 4: NS bifurcation visual depiction, MLEs and FDs diagram of species for changing parameter $\rho$

orbits, which include stable cycles of varying lengths. From an ecological perspective, this can be seen as the fluctuation between different population cycles, like the regular oscillations of prey and predator populations that have varying durations. By examining these models, we can acquire an understanding of the fundamental mechanisms that influence population cycles and other ecological processes and create more efficient approaches to enhance ecosystem stability and resilience.

Neimark-Sacker bifurcations are linked to the shift from periodic to quasi-periodic behaviour in dynamical systems. In ecological models, this could indicate a change from straightforward, consistent population cycles to more complex, non-repetitive patterns. The presence of Neimark-Sacker bifurcations leads to quasi-periodic oscillations in the ecological system. The oscillations do not repeat precisely, making interacting species' temporal dynamics more complex. In general, the Neimark-Sacker bifurcation in discrete prey-predator models emphasizes the significance of comprehending the dynamics of populations and their interactions in ecological systems. By studying these models, we can gain insight into the fundamental mechanisms that drive population cycles and other ecological processes and develop more effective strategies to improve ecosystem stability and resilience.

To sum up, period-doubling and Neimark-Sacker bifurcations in ecological models indicate changes in system behavior from straightforward and foreseeable to intricate and potentially disorderly dynamics. These divisions provide an understanding into the stability, robustness, and adaptation of ecological systems, highlighting the significance of addressing non-linear dynamics and bifurcation theory in the examination of population interactions.



2 Jan 2024 08:51:36 PST
231108-MdJasim Version 2 - Submitted to Rocky Mountain J. Math.

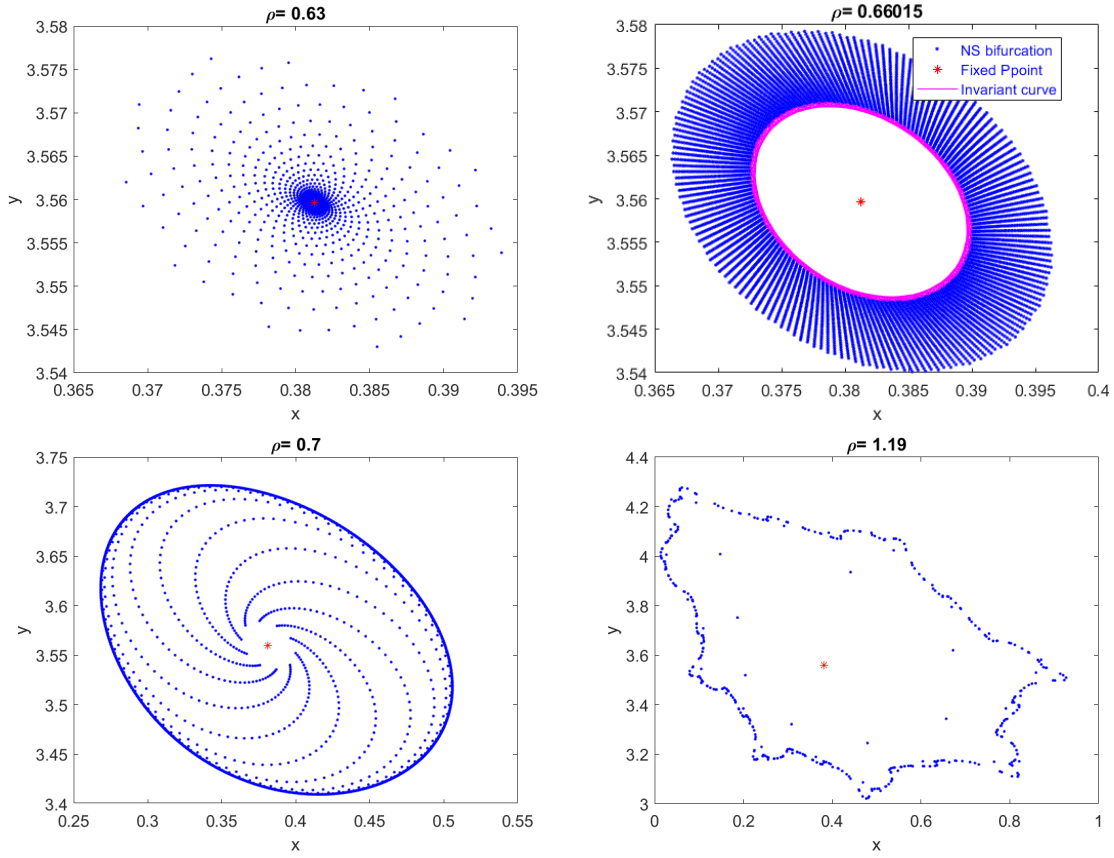


Figure 5: The phase diagram for altering the input of $\rho$

### 6.2 Fractal Dimension.

The chaotic attractors of a model are identified by its fractal dimensions (FD), which is measured by [9]

$$\widehat{FD}_{fd} = k + \frac{\sum_{j=1}^{k} \mathfrak{tt}_j}{|\mathfrak{tt}_{k+1}|} \tag{16}$$

In which $k$ is the largest integer number such that $\sum_{j=1}^{k} \mathfrak{tt}_j \geq 0$ and $\sum_{j=1}^{k+1} \mathfrak{tt}_j < 0$ and $\mathfrak{t}_j$'s are Lyapunov exponenets.

Now, the model (5) fractal dimensions structure is as follows:

$$\widehat{FD}_{fd} = 2 + \frac{\mathfrak{tt}_1}{|\mathfrak{tt}_2|} \tag{17}$$

Given that the model (5)'s chaotic dynamics (ref. Figure5) are measured using the FD sign (ref. Figure 4 (d)).

## 7 Chaos Management

In this section, we aim to apply Ott-Grebogi-Yorke (OGY) feedback control [40] and state feedback [35] approach to system (5) for preventing chaos at the positive fixed point of system (5) under the influence of Neimark-Sacker and Period-doubling bifurcation. In system (5), we write the OGY technique as follows:



2 Jan 2024 08:51:36 PST
231108-MdJasim Version 2 - Submitted to Rocky Mountain J. Math.

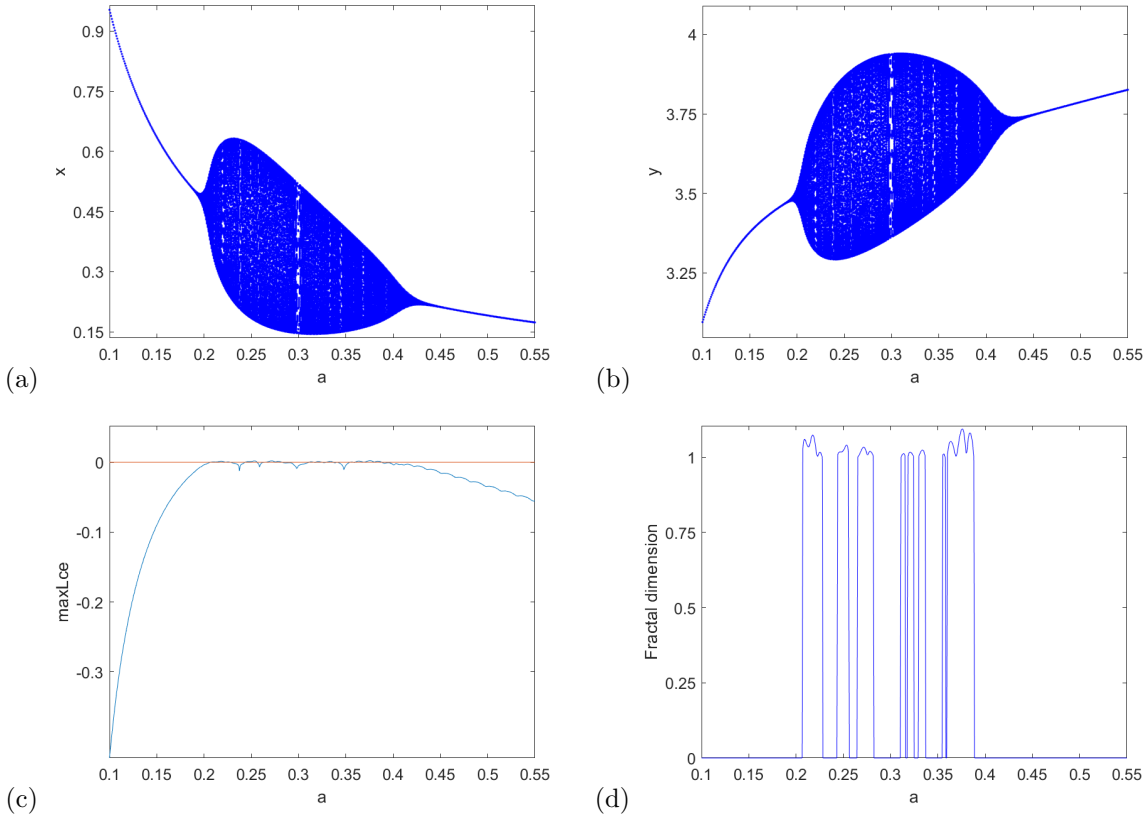


Figure 6: NS bifurcation visual depiction, MLEs and FDs diagram of species for changing parameter $a$

$$\begin{aligned} x_{n+1} &= x_n + \frac{\rho^\tau}{\Gamma(\tau+1)}\left(rx_n \ln\frac{k}{x_n} - \frac{\eta_c x_n}{\gamma_c + x_n} y_n\right) = g\tilde{b}_1(x,y,a), \\ y_{n+1} &= y_n + \frac{\rho^\tau}{\Gamma(\tau+1)}\left(\beta_c(1-e^{-ax_n})y_n - \delta_c y_n\right) = g\tilde{b}_2(x,y,a), \end{aligned} \tag{18}$$

where the chaos control parameter is taken to be $a$. Additionally, it is presummated that $a \in (a_0 - \delta_1, a_0 + \delta_1)$ with $\delta_1 > 0$ and $a_0$ denoting the nominal value of $a$. In the vicinity of the fixed point $\kappa_2(x^*, y^*)$, where $x^* = -\frac{\ln\left[1-\frac{\delta_c}{\beta_c}\right]}{a}, y^* = \frac{r(x^*+\gamma_c)\ln\left[\frac{k}{x^*}\right]}{\eta_c}$, one can then approximate system (18) as follows:

$$\begin{bmatrix} x_{n+1} - x^* \\ y_{n+1} - y^* \end{bmatrix} \approx \tilde{A_{cc}} \begin{bmatrix} x_n - x^* \\ y_n - y^* \end{bmatrix} + \tilde{B_{cc}}\left[a - a_0\right] \tag{19}$$

where

$$\begin{aligned} \tilde{A_{cc}} &= \begin{bmatrix} \frac{\partial g\tilde{b}_1(x,y,a)}{\partial x} & \frac{\partial g\tilde{b}_1(x,y,a)}{\partial y} \\ \frac{\partial g\tilde{b}_2(x,y,a)}{\partial x} & \frac{\partial g\tilde{b}_2(x,y,a)}{\partial y} \end{bmatrix} \\ &= \begin{bmatrix} 1 - r\tilde{\mu_b} + \frac{rx^*\ln\left[\frac{k}{x^*}\right]}{x^*+\gamma_c} & -\frac{x^*\eta_c\tilde{\mu_b}}{x^*+\gamma_c} \\ \frac{ae^{-ax^*}r\beta_c(x^*+\gamma_c)\tilde{\mu_b}\ln\left[\frac{k}{x^*}\right]}{\eta_c} & 1 - \delta_c\tilde{\mu_b} + \beta_c(1-e^{-ax^*})\tilde{\mu_b} \end{bmatrix} \end{aligned}$$

and

$$\tilde{B_{cc}} = \begin{bmatrix} \frac{\partial g\tilde{b}_1(x,y,a)}{\partial a} \\ \frac{\partial g\tilde{b}_2(x,y,a)}{\partial a} \end{bmatrix} = \begin{bmatrix} 0 \\ \frac{e^{-ax^*}rx^*\beta_c(x^*+\gamma_c)\tilde{\mu_b}\ln\left[\frac{k}{x^*}\right]}{\eta_c}. \end{bmatrix}$$

Additionally, the system (18) is managed by the matrix shown below:



2 Jan 2024 08:51:36 PST
231108-MdJasim Version 2 - Submitted to Rocky Mountain J. Math.

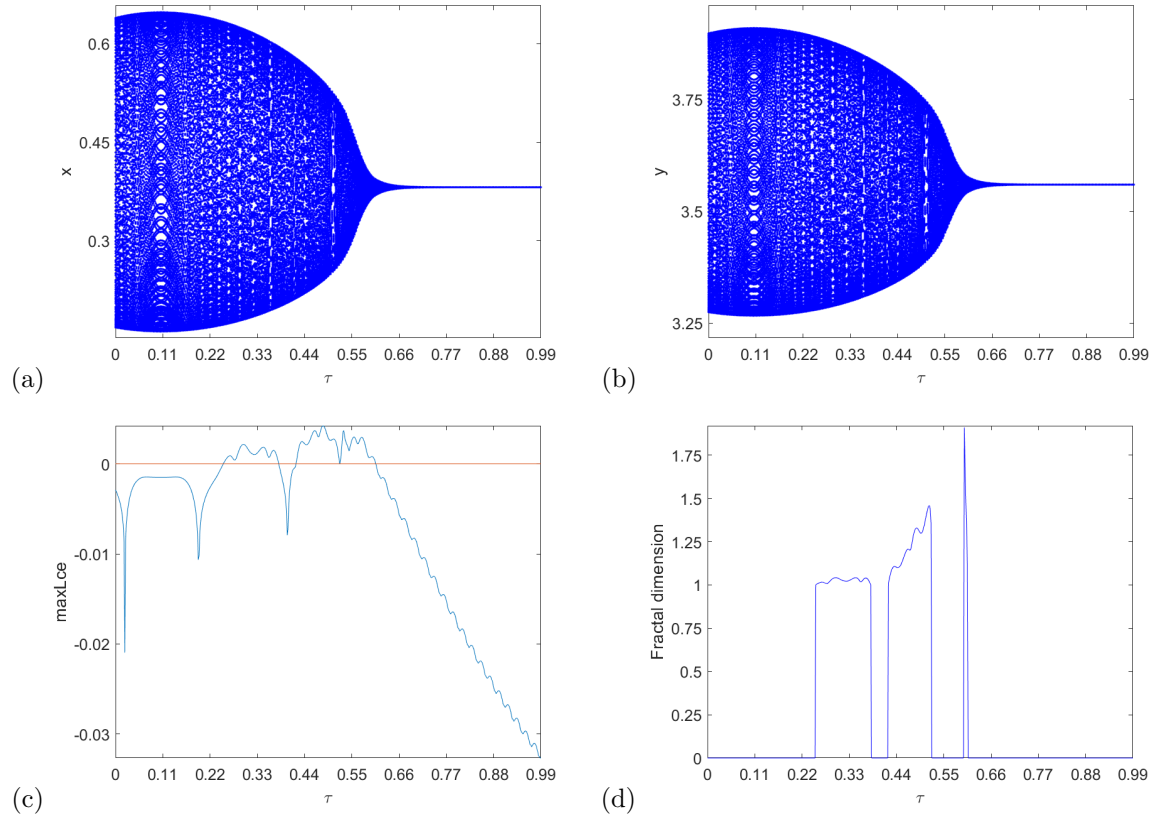


Figure 7: NS bifurcation visual depiction, MLEs and FDs diagram of species for changing parameter $\tau$

$$\tilde{C_{cc}} = \left[\tilde{B_{cc}} : \tilde{A_{cc}}\tilde{B_{cc}}\right] = \begin{bmatrix} 0 & -e^{-ax^*} r x^{*2} \beta_c \tilde{\mu_b}^2 \ln\left[\frac{k}{x^*}\right] \\ \frac{e^{-ax^*} r x^* \beta_c (x^* + \gamma_c)\tilde{\mu_b} \ln\left[\frac{k}{x^*}\right]}{\eta_c} & \frac{e^{-2ax^*} r x^* \beta_c (x^* + \gamma_c)\tilde{\mu_b}(-\beta_c - \tilde{\mu_b} + e^{ax^*}(1 + (\beta_c - \delta_c)\tilde{\mu_b})) \ln\left[\frac{k}{x^*}\right]}{\eta_c}. \end{bmatrix}$$

Therefore, it is simple to conclude that $\tilde{C_{cc}}$ has a rank of 2. We think that $[a - a_0] = -\tilde{K_{cc}} \begin{bmatrix} x_n - x^* \\ y_n - y^* \end{bmatrix}$ where $\tilde{K_{cc}} = [\tilde{\sigma_{c1}} \quad \tilde{\sigma_{c2}}]$, then system (18) becomes

$$\begin{bmatrix} x_{n+1} - x^* \\ y_{n+1} - y^* \end{bmatrix} \approx [\tilde{A_{cc}} - \tilde{B_{cc}}\tilde{K_{cc}}] \begin{bmatrix} x_n - x^* \\ y_n - y^*. \end{bmatrix}$$

Additionally, system (5) offers the appropriate controlled system.

$$\begin{aligned} x_{n+1} &= x_n + \frac{\rho^\tau}{\Gamma(\tau+1)} \left( r x_n \ln \frac{k}{x_n} - \frac{\eta_c x_n}{\gamma_c + x_n} y_n \right), \\ y_{n+1} &= y_n + \frac{\rho^\tau}{\Gamma(\tau+1)} \left( \beta_c (1 - e^{-(a_0 - \tilde{\sigma_{c1}}(x_n - x^*) - \tilde{\sigma_{c2}}(y_n - y^*))x_n}) y_n - \delta_c y_n \right) \end{aligned} \tag{20}$$

.

If both eigenvalues of $(\tilde{A_{cc}} - \tilde{B_{cc}}\tilde{K_{cc}})$ occupy a space inside a unit disk which is open, the fixed point $(x^*, y^*)$ is also locally asymptotically stable.

Also,



2 Jan 2024 08:51:36 PST
231108-MdJasim Version 2 - Submitted to Rocky Mountain J. Math.

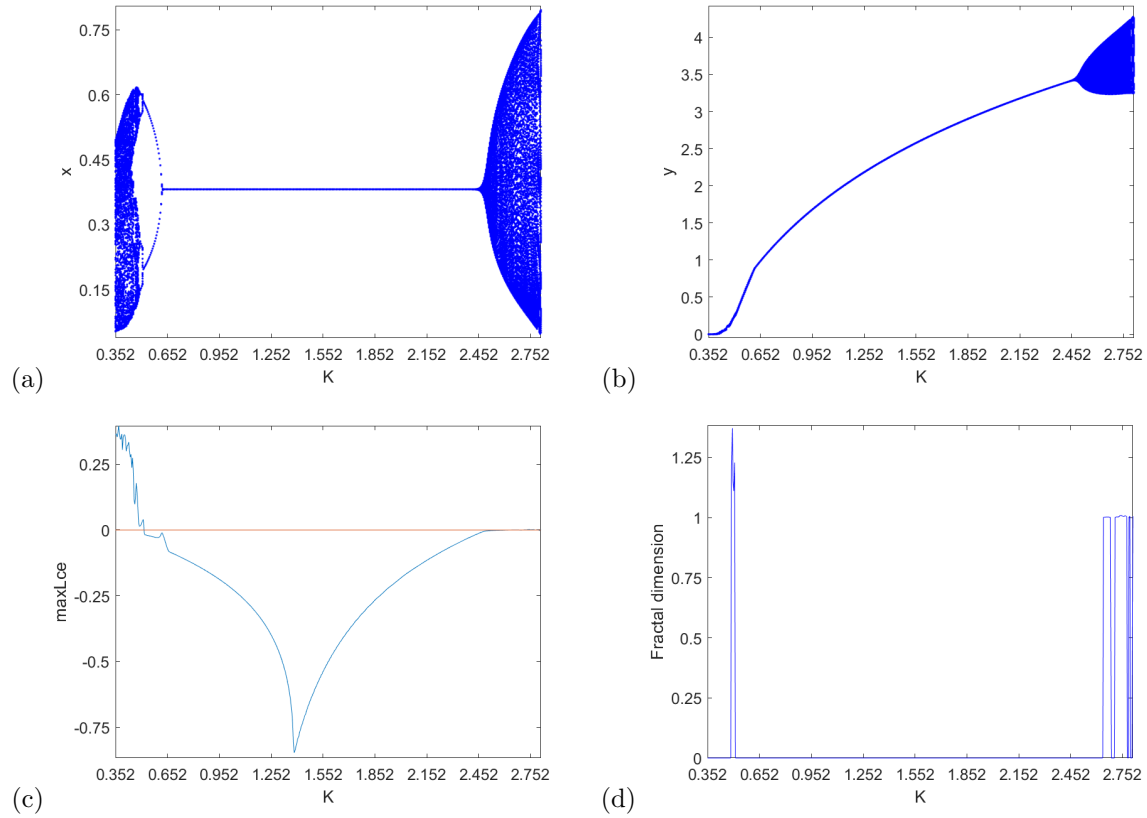


Figure 8: NS bifurcation visual depiction, MLEs and FDs diagram of species for changing parameter $k$

$$\tilde{A_{cc}} - \tilde{B_{cc}}\tilde{K_{cc}} = \begin{bmatrix} \tilde{b_{11}} & \tilde{b_{12}} \\ \tilde{b_{21}} & \tilde{b_{22}} \end{bmatrix}$$

where

$$\tilde{b_{11}} = 1 + \left( -r + \frac{rx^* \ln\left[\frac{k}{x^*}\right]}{x^* + \gamma_c} \right) \tilde{\mu_b}$$

$$\tilde{b_{12}} = -\frac{x^* \eta_c \tilde{\mu_b}}{x^* + \gamma_c}$$

$$\tilde{b_{21}} = \frac{ae^{-ax^*} r\beta_c(x^* + \gamma_c)\tilde{\mu_b} \ln\left[\frac{k}{x^*}\right]}{\eta_c} - \frac{e^{-ax^*} rx^* \beta_c(x^* + \gamma_c)\tilde{\mu_b} \ln\left[\frac{k}{x^*}\right]\tilde{\sigma_{c1}}}{\eta_c}$$

$$\tilde{b_{22}} = 1 + \left( (1 - e^{-ax^*})\beta_c - \delta_c \right) \tilde{\mu_b} - \frac{e^{-ax^*} rx^* \beta_c(x^* + \gamma_c)\tilde{\mu_b} \ln\left[\frac{k}{x^*}\right]\tilde{\sigma_{c2}}}{\eta_c}$$

Furthermore,

$$\tilde{\lambda_c}^2 - \tilde{\Lambda_{cc}}\lambda_c + \tilde{F_{cc}} = 0 \tag{21}$$

where

$$\begin{aligned} \tilde{\Lambda_{cc}} &= \tilde{b_{11}} + \tilde{b_{22}} \\ \tilde{F_{cc}} &= \tilde{b_{11}}\tilde{b_{22}} - \tilde{b_{12}}\tilde{b_{21}} \end{aligned} \tag{22}$$

It is thus possible to solve the equations $\lambda_{c1} = \pm 1$ and $\lambda_{c1}\lambda_{c2} = 1$ to obtain the lines of marginal stability. The open unit disc has both eigenvalues guarantee to these restrictions as well. We find the following equations from (21), taking into account the cases $\lambda_{c1}\lambda_{c2} = 1$, $\lambda_{c1} = -1$ and $\lambda_{c1} = 1$ successively.



2 Jan 2024 08:51:36 PST
231108-MdJasim Version 2 - Submitted to Rocky Mountain J. Math.

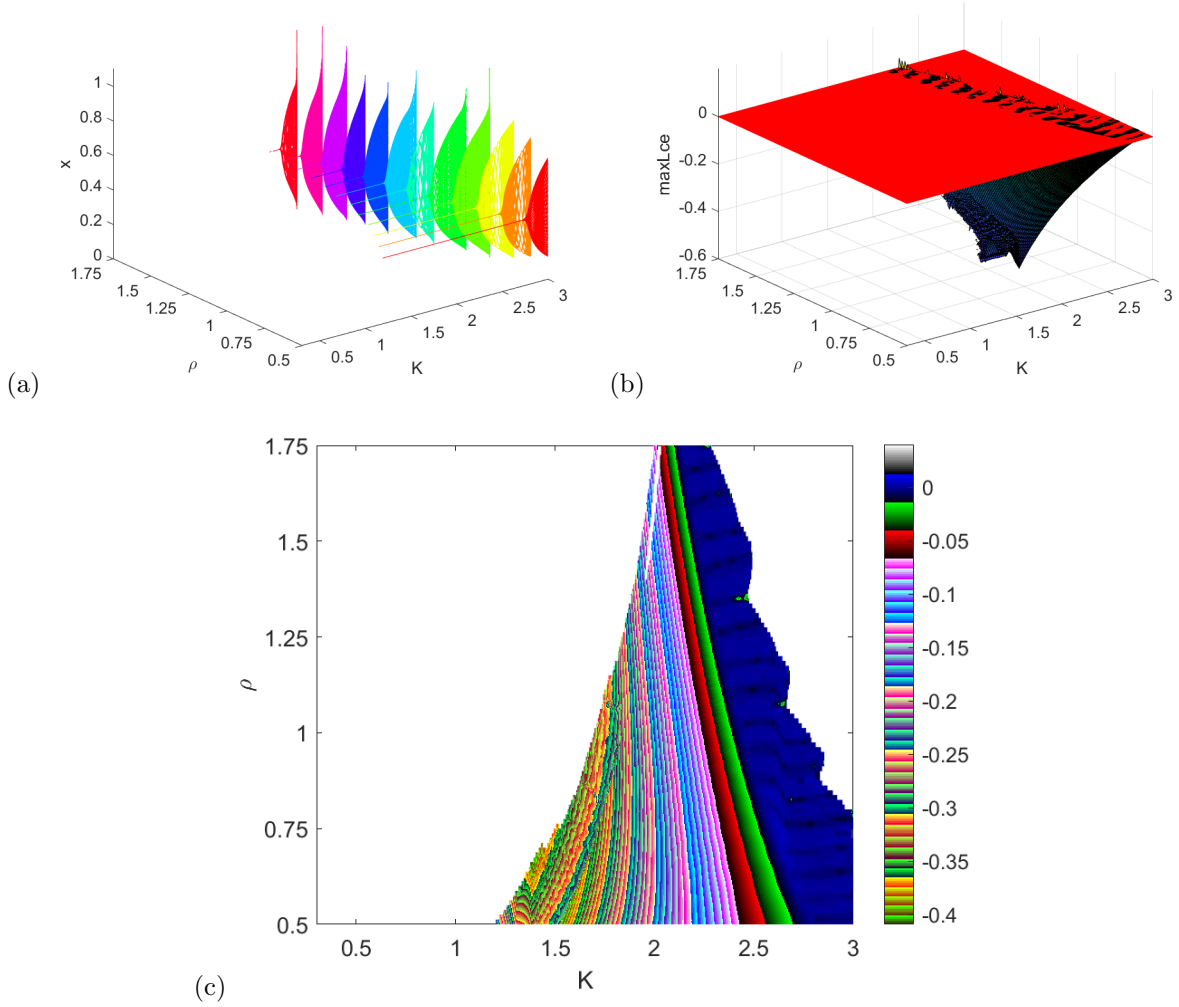


Figure 9: (a) Diagram of bifurcation in $(k, \rho, x)$ (b) 2D projection of 3D MLP (c) MLPs projected in two dimensions onto the $(k, \rho)$ plane

$$L_{c1} = \tilde{F_{cc}} - 1,$$
$$L_{c2} = \tilde{\Lambda_{cc}} - \tilde{F_{cc}} - 1,$$
$$L_{c3} = 1 + \tilde{\Lambda_{cc}} + \tilde{F_{cc}}.$$

Therefore, the stability zone for (18) is a triangle in the $\tilde{\sigma_{c1}}, \tilde{\sigma_{c2}}$-plane that is surrounded by $L_{c1}, L_{c2}$ and $L_{c3}$.

The unstable routes of the system (5) begin at this point, and chaos is stabilized using a technique called state feedback control. It is possible to manipulate the system (5) to take on a specific form, using the formula below and adding a feedback controlling force $u_{cc}$.

$$\begin{aligned} x_{n+1} &= x_n + \frac{\rho^\tau}{\Gamma(\tau+1)}\left(r x_n \ln\frac{k}{x_n} - \frac{\eta_c x_n}{\gamma_c + x_n} y_n\right) + u_{cc} \\ y_{n+1} &= y_n + \frac{\rho^\tau}{\Gamma(\tau+1)}\left(\beta_c(1 - e^{-a x_n}) y_n - \delta_c y_n\right) \\ u_{cc} &= -k_1(x_n - x^*) - k_2(y_n - y^*) \end{aligned} \tag{23}$$



2 Jan 2024 08:51:36 PST
231108-MdJasim Version 2 - Submitted to Rocky Mountain J. Math.

where the system (5)'s nonnegative equilibrium point is represented by $(x^*, y^*)$. The feedback gains are represented by the values $k_1$ and $k_2$.

**Scenario (iii):** To discuss the OGY feedback control mechanism of the system (5), we first set $(r, k, a_0, \eta, \beta, \delta, \gamma, \tau, \rho) = (2.5, 2.65, 0.35, 1.2, 1.1, 0.1, 0.5, 0.6, 0.8)$. In this instance, the unstable system (5) has a single non-negative fixed point $(x^*, y^*) = (0.272315, 3.66102)$. Then, depending on these parametric parameters, we give the controlled system below.

$$\begin{aligned} x_{n+1} &= x_n + 0.9789\left(2.5x_n \ln\frac{2.65}{x_n} - \frac{1.2x_n}{0.5+x_n}y_n\right), \\ y_{n+1} &= y_n + 0.9789\left(1.1(1 - e^{-(0.35-\tilde{\sigma_{c1}}(x_n-x^*)-\tilde{\sigma_{c2}}(y_n-y^*))x_n})y_n - 0.1y_n\right), \end{aligned} \tag{24}$$

.

where $\tilde{K} = [\tilde{\sigma_{b1}} \quad \tilde{\sigma_{b2}}]$. We also get,

$$\tilde{A_{cc}} = \begin{bmatrix} 0.516131 & -0.414187 \\ 1.25432 & 1 \end{bmatrix},$$

$$\tilde{B_{cc}} = \begin{bmatrix} 0 \\ 0.975915 \end{bmatrix},$$

$$\tilde{C_{cc}} = \begin{bmatrix} 0 & -0.414187 \\ 0.975915 & 0.975915 \end{bmatrix}.$$

The rank of the $\tilde{C_{cc}}$ matrix being 2 may then be easily verified. As a result, the system (24) may be controlled and give the Jacobian matrix of the managed system.

$$\tilde{A_{cc}} - \tilde{B_{cc}}\tilde{K_{cc}} = \begin{bmatrix} 0.516131 & -0.414187 \\ 1.25432 - 0.975915\tilde{\sigma_{c1}} & 10.975915\tilde{\sigma_{c2}} \end{bmatrix}.$$

The lines of marginal stability in this instance are provided by

$$\begin{aligned} L_{c1} &= 0.0356548 - 0.404211\tilde{\sigma_{c1}} - 0.5037\tilde{\sigma_{c2}} = 0, \\ L_{c2} &= 0.519524 - 0.404211\tilde{\sigma_{c1}} + 0.472215\tilde{\sigma_{c2}} = 0, \\ L_{c3} &= -3.55179 + 0.404211\tilde{\sigma_{c1}} + 1.47962\tilde{\sigma_{c2}} = 0. \end{aligned}$$

The regulated system(24)'s stable triangular zone defined by the marginal lines $L_{c1}, L_{c2}$ and $L_{c3}$ is thus depicted in Figure 10.

We ran numerical simulations to investigate how the SFC performs (see Figure 10). With the exception of $\rho = 1.19$, the others will remain the same as in OGY method. The chosen feedback gains are $k_1 = 0.3$ and $k_2 = -0.12$ respectively.

# 8 Conclusions

The dynamics of a discrete prey-predator model with mixed functional response in fractional order are investigated in this study. Under precise parametric conditions, two fixed points are found, also the paper investigated the details about their stability. We also show numerically and theoretically that the system



**2 Jan 2024 08:51:36 PST**
**231108-MdJasim Version 2 - Submitted to Rocky Mountain J. Math.**

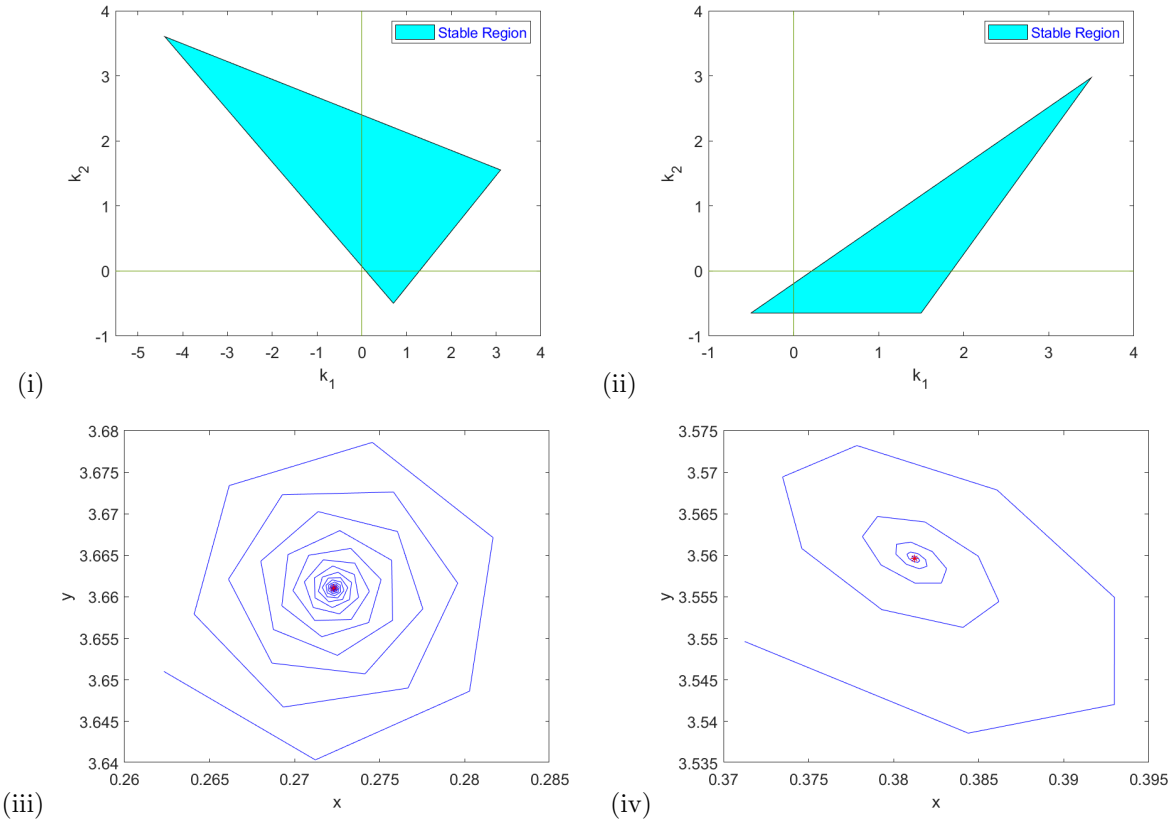


Figure 10: (i-ii) OGY method and State feedback method's stable region (iii-iv) Trajectories of a stable system

can experience PD and NS bifurcations under specific circumstances. Notably, our results show that the model exhibits chaotic behavior and that the system becomes unstable when the parameter $\rho$ increases, causing a change from an orderly state to a chaotic one. Also, we observe some more interesting bifurcation diagrams when the parameters $a, k$ increase. Additionally, numerical simulations using Matlab are carried out to show the theoretical observations in the form of phase portraits, maximal Lyapunov exponents, Fractal dimensions and bifurcation diagrams. We also show, numerically and analytically, how the OGY and state feedback strategies can be used to manage chaotic behavior. Unique bifurcations from different perspectives demonstrate the discrete model dynamics at different levels of complexity. As an illustration, the Neimark-Sacker bifurcation sets off a chain reaction that eventually results in complicated dynamics, by creating a dynamic transition from a stable fixed point to appealing cycles, such as periodic windows and chaotic attractors, which are made more appealing. Environmental changes may cause populations that have irregular oscillations to suddenly transition to regular oscillations. Important information about the behavior of nonlinear dynamical systems nearing the critical point can be gleaned from the curve in the supercritical NS bifurcation which is invariant. It is vital to comprehend the change from simple and orderly dynamics to more complicated and chaotic dynamics because it demonstrates how the system responds to changes in a parameter. Pairwise coexistence and self-reproduction between predator and prey populations is suggested by a closed curve (invariant) for supercritical NS in ecology. There may be periodic or quasi-periodic dynamics on the invariant curve. The bifurcation with a period-doubling is how



2 Jan 2024 08:51:36 PST
231108-MdJasim Version 2 - Submitted to Rocky Mountain J. Math.

the model depicts the evolution of species. The transformation of a steady periodic solution into chaotic behavior is related to the period-doubling bifurcation. It serves as an example of the variety of irregular behavior in a variety of inborn systems and phenomena.

Our key discovery is that the amount of memory represented by the parameter $\tau$ considerably influences the system's behavior. By our research, a feeble memory is represented by a $\tau$ value that tends to 1, which leads to chaotic behavior, whereas a stiff memory denoted by a $\tau \approx 0$, freezes the system. These findings show how memory is essential to the behavior of the model. This paper provides a thorough analysis of the model's dynamics and illustrates how bifurcations and chaos might develop in specific parametric situations. We further emphasize the influence of memory on system behavior. Our research enlightens the preface that memory works in the model dynamics and adds to our understanding of the dynamics of the model.

## Future Work

In the future, there are multiple potential areas for further research in this field. The dynamics of predator-prey systems can be significantly influenced by additional factors such as spatial heterogeneity and environmental stochasticity. These elements provide intricacy and authenticity to ecological models, enabling a more precise portrayal of real-life ecosystems. Including these aspects in predator-prey models necessitates more intricate mathematical formulations and computer methodologies. Scientists frequently utilize models that incorporate spatial information or probabilistic equations to simulate the behavior of ecological systems when affected by variations in space and random environmental factors. These models assist in understanding the complex relationships that take place in actual ecosystems and offer insights into the potential of predator and prey populations to recover and remain stable. Our conclusion summarises the main findings of our research and suggests future research options. It highlights the possibilities for further inquiry and application in the field of predator-prey dynamics by addressing the significant outcomes of our study.

## Funding

There is no funding for this study.

## Data Availability Statement

There are no related data for this manuscript.

## Competing interests

The authors claim that there are no conflicting interests.

## Authors' contributions

The main findings were verified by all authors, who also gave their unanimous approval to the final manuscript.

## References


[1] Abdelaziz, M. A., Ismail, A. I., Abdullah, F. A. & Mohd, M. H. [2018] "Bifurcations and chaos in a discrete si epidemic model with fractional order," *Advances in Difference Equations* **2018**, 1–19.

[2] Ahmad, W. M. & Sprott, J. C. [2003] "Chaos in fractional-order autonomous nonlinear systems," *Chaos, Solitons & Fractals* **16**, 339–351.

[3] Al-Kaff, M. O., El-Metwally, H. A. & Elabbasy, E.-M. M. [2022] "Qualitative analysis and phase of chaos control of the predator-prey model with holling type-iii," *Scientific Reports* **12**, 20111.

[4] Arditi, R. & Ginzburg, L. R. [1989] "Coupling in predator-prey dynamics: ratio-dependence," *Journal of theoretical biology* **139**, 311–326.

[5] Balcı, E., Öztürk, İ. & Kartal, S. [2019] "Dynamical behaviour of fractional order tumor model with caputo and conformable fractional derivative," *Chaos, Solitons & Fractals* **123**, 43–51.

[6] Bilal Ajaz, M., Saeed, U., Din, Q., Ali, I. & Israr Siddiqui, M. [2020] "Bifurcation analysis and chaos control in discrete-time modified leslie–gower prey harvesting model," *Advances in Difference Equations* **2020**, 1–24.

[7] Caputo, M. [1967] "Linear models of dissipation whose q is almost frequency independentii," *Geophysical Journal International* **13**, 529–539.

[8] Caputo, M. & Mainardi, F. [1971] "A new dissipation model based on memory mechanism," *Pure and applied Geophysics* **91**, 134–147.

[9] Cartwright, J. H. [1999] "Nonlinear stiffness, lyapunov exponents, and attractor dimension," *Physics Letters A* **264**, 298–302.

[10] Cheng, L. & Cao, H. [2016] "Bifurcation analysis of a discrete-time ratio-dependent predator–prey model with allee effect," *Communications in Nonlinear Science and Numerical Simulation* **38**, 288–302.

[11] Cosner, C., DeAngelis, D. L., Ault, J. S. & Olson, D. B. [1999] "Effects of spatial grouping on the functional response of predators," *Theoretical population biology* **56**, 65–75.

[12] Danca, M., Codreanu, S. & Bako, B. [1997] "Detailed analysis of a nonlinear prey-predator model," *Journal of biological physics* **23**, 11.

[13] De Oliveira, E. C. & Tenreiro Machado, J. A. [2014] "A review of definitions for fractional derivatives and integral," *Mathematical Problems in Engineering* **2014**.

[14] Din, Q. [2017] "Complexity and chaos control in a discrete-time prey-predator model," *Communications in Nonlinear Science and Numerical Simulation* **49**, 113–134.

[15] Din, Q. [2017] "Global stability of beddington model," *Qualitative theory of dynamical systems* **16**, 391–415.

[16] Din, Q., Donchev, T. & Kolev, D. [2018] "Stability, bifurcation analysis and chaos control in chlorine dioxide–iodine–malonic acid reaction," *MATCH Commun. Math. Comput. Chem* **79**, 577–606.

[17] Du, M., Wang, Z. & Hu, H. [2013] "Measuring memory with the order of fractional derivative," *Scientific reports* **3**, 3431.

[18] Elettreby, M., Nabil, T. & Khawagi, A. [2020] "Stability and bifurcation analysis of a discrete predator-prey model with mixed holling interaction," *Computer Modeling in Engineering & Sciences* **122**, 907–922.

[19] Elettreby, M. F., Khawagi, A. & Nabil, T. [2019] "Dynamics of a discrete prey–predator model with mixed functional response," *International Journal of Bifurcation and Chaos* **29**, 1950199.

[20] Elsadany, A. & Matouk, A. [2015] "Dynamical behaviors of fractional-order lotka–volterra predator–prey model and its discretization," *Journal of Applied Mathematics and Computing* **49**, 269–283.

[21] Fan, M. & Kuang, Y. [2004] "Dynamics of a nonautonomous predator–prey system with the beddington–deangelis functional response," *Journal of Mathematical Analysis and applications* **295**, 15–39.

[22] Guckenheimer, J. & Holmes, P. [2013] *Nonlinear oscillations, dynamical systems, and bifurcations of vector fields*, Vol. 42 (Springer Science & Business Media).

[23] Hadeler, K. & Gerstmann, I. [1990] "The discrete rosenzweig model," *Mathematical Biosciences* **98**, 49–72.

[24] Hastings, A., Hom, C. L., Ellner, S., Turchin, P. & Godfray, H. C. J. [1993] "Chaos in ecology: is mother nature a strange attractor?" *Annual review of ecology and systematics* **24**, 1–33.

[25] Holling, C. S. [1965] "The functional response of predators to prey density and its role in mimicry and population regulation," *The Memoirs of the Entomological Society of Canada* **97**, 5–60.

[26] Hu, D. & Cao, H. [2015] "Bifurcation and chaos in a discrete-time predator–prey system of holling and leslie type," *Communications in Nonlinear Science and Numerical Simulation* **22**, 702–715.

[27] Ishaque, W., Din, Q., Taj, M. & Iqbal, M. A. [2019] "Bifurcation and chaos control in a discrete-time predator–prey model with nonlinear saturated incidence rate and parasite interaction," *Advances in Difference Equations* **2019**, 1–16.

[28] Ivlev, V. [1961] "Experimental ecology of the feeding of fishes yale university press new haven connecticut," .



**2 Jan 2024 08:51:36 PST**
**231108-MdJasim Version 2 - Submitted to Rocky Mountain J. Math.**

[29] Khan, M. A. [2019] "Chaotic behavior of harvesting leslie-gower predator-prey model," *Computational Ecology and Software* **9**, 67.

[30] Khan, M. S. [2022] "Bifurcation analysis of a discrete-time four-dimensional cubic autocatalator chemical reaction model with coupling through uncatalysed reactant," *MATCH Commun. Math. Comput. Chem* **87**, 415–439.

[31] Khan, M. S., Samreen, M., Gómez-Aguilar, J. & Pérez-Careta, E. [2022] "On the qualitative study of a discrete-time phytoplankton-zooplankton model under the effects of external toxicity in phytoplankton population," *Heliyon* **8**, e12415.

[32] Liu, B., Zhang, Y. & Chen, L. [2005] "Dynamic complexities in a lotka–volterra predator–prey model concerning impulsive control strategy," *International Journal of Bifurcation and Chaos* **15**, 517–531.

[33] Liu, X. & Xiao, D. [2007] "Complex dynamic behaviors of a discrete-time predator–prey system," *Chaos, Solitons & Fractals* **32**, 80–94.

[34] Lotka, A. J. [1925] *Elements of physical biology* (Williams & Wilkins).

[35] Lynch, S. *et al.* [2007] *Dynamical systems with applications using Mathematica®* (Springer).

[36] Machado, J. T., Kiryakova, V. & Mainardi, F. [2011] "Recent history of fractional calculus," *Communications in nonlinear science and numerical simulation* **16**, 1140–1153.

[37] Meral, F., Royston, T. & Magin, R. [2010] "Fractional calculus in viscoelasticity: an experimental study," *Communications in nonlinear science and numerical simulation* **15**, 939–945.

[38] Naik, P. A., Eskandari, Z., Avazzadeh, Z. & Zu, J. [2022] "Multiple bifurcations of a discrete-time prey–predator model with mixed functional response," *International Journal of Bifurcation and Chaos* **32**, 2250050.

[39] Nicholson, A. J. [1957] "The self-adjustment of populations to change," *Cold spring harbor symposia on quantitative biology* (Cold Spring Harbor Laboratory Press), pp. 153–173.

[40] Ott, E., Grebogi, C. & Yorke, J. A. [1990] "Controlling chaos," *Physical review letters* **64**, 1196.

[41] Rana, S. & Kulsum, U. [2017] "Bifurcation analysis and chaos control in a discrete-time predator-prey system of leslie type with simplified holling type iv functional response," *Discrete Dynamics in Nature and Society* **2017**.

[42] Rana, S. M. S., Uddin, M. J., Santra, P., Mahapatra, G. *et al.* [2023] "Chaotic dynamics and control of a discrete-time chen system," *Mathematical Problems in Engineering* **2023**.

[43] Salman, S., Yousef, A. & Elsadany, A. [2016] "Stability, bifurcation analysis and chaos control of a discrete predator-prey system with square root functional response," *Chaos, Solitons & Fractals* **93**, 20–31.

[44] Shabbir, M. S., Din, Q., Safeer, M., Khan, M. A. & Ahmad, K. [2019] "A dynamically consistent nonstandard finite difference scheme for a predator–prey model," *Advances in Difference Equations* **2019**, 1–17.

[45] Singh, A., Elsadany, A. A. & Elsonbaty, A. [2019] "Complex dynamics of a discrete fractional-order leslie-gower predator-prey model," *Mathematical Methods in the Applied Sciences* **42**, 3992–4007.

[46] Sun, H. & Cao, H. [2007] "Bifurcations and chaos of a delayed ecological model," *Chaos, Solitons & Fractals* **33**, 1383–1393.

[47] Sun, Y., Zhao, M. & Du, Y. [2023] "Bifurcations, chaos analysis and control in a discrete predator–prey model with mixed functional responses," *International Journal of Biomathematics* , 2350028.

[48] Sun, Y., Zhao, M. & Du, Y. [2024] "Bifurcations, chaos analysis and control in a discrete predator–prey model with mixed functional responses," *International Journal of Biomathematics* **17**, 2350028.

[49] Uddin, M. J., Rana, S. M. S., Işık, S. & Kangalgil, F. [2023] "On the qualitative study of a discrete fractional order prey–predator model with the effects of harvesting on predator population," *Chaos, Solitons & Fractals* **175**, 113932.

[50] Uddin, M. J. & Rana, S. S. [2023] "Chaotic dynamics of the fractional order schnakenberg model and its control," *Mathematics in Applied Sciences and Engineering* , 1–21.

[51] Velasco, M. P., Usero, D., Jiménez, S., Vázquez, L., Vázquez-Poletti, J. L. & Mortazavi, M. [2020] "About some possible implementations of the fractional calculus," *Mathematics* **8**, 893.

[52] Volterra, V. [1927] *Variazioni e fluttuazioni del numero d'individui in specie animali conviventi*, Vol. 2 (Societá anonima tipografica" Leonardo da Vinci").

[53] Xu, Z. & Chen, W. [2013] "A fractional-order model on new experiments of linear viscoelastic creep of hami melon," *Computers & Mathematics with Applications* **66**, 677–681.

[54] Zhang, Y., Zhang, Q., Zhao, L. & Yang, C. [2007] "Dynamical behaviors and chaos control in a discrete functional response model," *Chaos, Solitons & Fractals* **34**, 1318–1327.



**2 Jan 2024 08:51:36 PST**
**231108-MdJasim Version 2 - Submitted to Rocky Mountain J. Math.**